US009510763B2

(12) **United States Patent**
Ghosh et al.

(10) **Patent No.: US 9,510,763 B2**
(45) **Date of Patent: Dec. 6, 2016**

(54) **ASSESSING INTRA-CARDIAC ACTIVATION PATTERNS AND ELECTRICAL DYSSYNCHRONY**

(75) Inventors: **Subham Ghosh**, Circle Pines, MN (US); **Jeffrey M. Gillberg**, Coon Rapids, MN (US); **Robert W. Stadler**, Shoreview, MN (US)

(73) Assignee: **Medtronic, Inc.**, Minneapolis, MN (US)

(*) Notice: Subject to any disclaimer, the term of this patent is extended or adjusted under 35 U.S.C. 154(b) by 0 days.

(21) Appl. No.: **13/462,404**

(22) Filed: **May 2, 2012**

(65) **Prior Publication Data**

US 2012/0283587 A1 Nov. 8, 2012

Related U.S. Application Data

(60) Provisional application No. 61/482,053, filed on May 3, 2011.

(51) **Int. Cl.**
A61B 5/04 (2006.01)
A61B 5/0452 (2006.01)
(Continued)

(52) **U.S. Cl.**
CPC ***A61B 5/04012*** (2013.01); ***A61B 5/02*** (2013.01); ***A61B 5/0402*** (2013.01);
(Continued)

(58) **Field of Classification Search**
CPC A61B 5/0485; A61B 5/046–5/0472; A61N 1/0484; A61N 1/0476; A61N 1/3627; A61N 1/3682; A61N 1/3684
(Continued)

(56) **References Cited**

U.S. PATENT DOCUMENTS

4,233,987 A 11/1980 Feingold
4,402,323 A 9/1983 White
(Continued)

FOREIGN PATENT DOCUMENTS

CN 1043621 A 7/1990
CN 1253761 5/2000
(Continued)

OTHER PUBLICATIONS

(PCT/US2012/036302) PCT Notification of Transmittal of the International Search Report and the Written Opinion of the International Searching Authority.
(Continued)

Primary Examiner — Mallika D Fairchild
(74) *Attorney, Agent, or Firm* — Carol F. Barry

(57) **ABSTRACT**

Techniques for evaluating cardiac electrical dyssynchrony are described. In some examples, an activation time is determined for each of a plurality of torso-surface potential signals. The dispersion or sequence of these activation times may be analyzed or presented to provide variety of indications of the electrical dyssynchrony of the heart of the patient. In some examples, the locations of the electrodes of the set of electrodes, and thus the locations at which the torso-surface potential signals were sensed, may be projected on the surface of a model torso that includes a model heart. The inverse problem of electrocardiography may be solved to determine electrical activation times for regions of the model heart based on the torso-surface potential signals sensed from the patient.

32 Claims, 12 Drawing Sheets

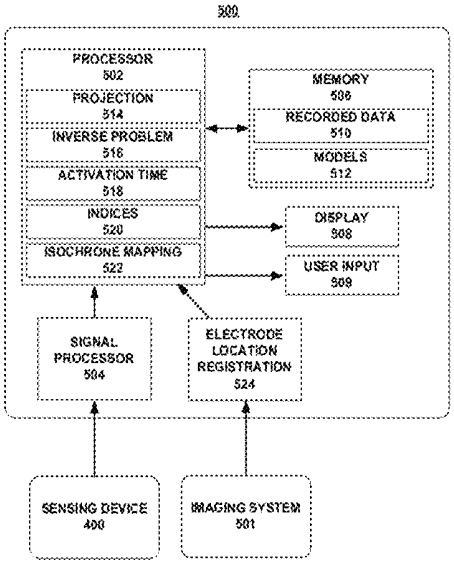

(51) **Int. Cl.**

A61B 5/05	(2006.01)
A61B 5/02	(2006.01)
A61B 5/0402	(2006.01)
A61B 5/0408	(2006.01)
A61N 1/04	(2006.01)
A61N 1/362	(2006.01)
A61N 1/368	(2006.01)
A61B 5/00	(2006.01)

(52) **U.S. Cl.**

CPC ***A61B 5/0452*** (2013.01); ***A61B 5/04085*** (2013.01); ***A61B 5/05*** (2013.01); ***A61B 5/742*** (2013.01); ***A61N 1/0476*** (2013.01); ***A61N 1/0484*** (2013.01); ***A61N 1/3627*** (2013.01); ***A61N 1/3682*** (2013.01); ***A61N 1/3684*** (2013.01)

(58) **Field of Classification Search**

USPC 600/508–510, 523, 525

See application file for complete search history.

(56) **References Cited**

U.S. PATENT DOCUMENTS

4,428,378	A		1/1984	Anderson et al.
4,497,326	A		2/1985	Curry
4,566,456	A		1/1986	Koning et al.
4,593,702	A		6/1986	Kepski
4,674,511	A		6/1987	Cartmell
4,763,660	A		8/1988	Kroll et al.
4,777,955	A		10/1988	Brayten et al.
4,787,389	A		11/1988	Tarjan
5,052,388	A		10/1991	Sivula et al.
5,054,496	A	*	10/1991	Wen et al. 600/509
5,311,873	A	*	5/1994	Savard et al. 600/508
5,331,960	A		7/1994	Lavine
5,334,220	A		8/1994	Sholder
5,443,492	A		8/1995	Stokes et al.
5,485,849	A		1/1996	Panescu et al.
5,514,163	A		5/1996	Markowitz et al.
5,552,645	A		9/1996	Weng
5,628,778	A		5/1997	Kruse et al.
5,671,752	A		9/1997	Sinderby et al.
5,683,429	A		11/1997	Mehra
5,683,432	A		11/1997	Goedeke et al.
5,687,737	A		11/1997	Branham et al.
5,810,740	A		9/1998	Paisner
5,876,336	A		3/1999	Swanson et al.
5,891,045	A		4/1999	Albrecht et al.
5,922,014	A		7/1999	Warman et al.
6,055,448	A		4/2000	Anderson et al.
6,128,535	A		10/2000	Maarse et al.
6,141,588	A		10/2000	Cox et al.
6,187,032	B1		2/2001	Ohyu et al.
6,205,357	B1		3/2001	Ideker et al.
6,226,542	B1		5/2001	Reisfeld
6,236,883	B1		5/2001	Ciaccio et al.
6,243,603	B1		6/2001	Ideker et al.
6,246,898	B1		6/2001	Vesely et al.
6,301,496	B1		10/2001	Reisfeld
6,311,089	B1		10/2001	Mann et al.
6,330,476	B1		12/2001	Ben-Ham et al.
6,358,214	B1		3/2002	Tereschouk
6,377,856	B1		4/2002	Carson
6,381,493	B1		4/2002	Stadler et al.
6,393,316	B1		5/2002	Gillberg et al.
6,418,346	B1		7/2002	Nelson et al.
6,442,433	B1		8/2002	Linberg
6,456,867	B2		9/2002	Reisfeld
6,473,638	B2		10/2002	Ferek-Petric
6,480,745	B2		11/2002	Nelson et al.
6,484,118	B1		11/2002	Govari
6,507,756	B1		1/2003	Heynen et al.
6,532,379	B2		3/2003	Stratbucker
6,584,343	B1		6/2003	Ransbury et al.
6,599,250	B2		7/2003	Webb et al.
6,625,482	B1		9/2003	Panescu et al.
6,640,136	B1		10/2003	Helland et al.
6,650,927	B1		11/2003	Keidar
6,766,189	B2		7/2004	Yu et al.
6,772,004	B2	*	8/2004	Rudy 600/509
6,804,555	B2		10/2004	Warkentin
6,847,836	B1		1/2005	Sujdak
6,856,830	B2		2/2005	He
6,882,882	B2		4/2005	Struble et al.
6,885,889	B2		4/2005	Chinchoy
6,915,149	B2		7/2005	Ben-Haim
6,968,237	B2		11/2005	Doan et al.
6,975,900	B2		12/2005	Rudy et al.
6,978,184	B1		12/2005	Marcus et al.
6,980,675	B2		12/2005	Evron et al.
7,016,719	B2		3/2006	Rudy et al.
7,031,777	B2		4/2006	Hine et al.
7,058,443	B2		6/2006	Struble
7,092,759	B2		8/2006	Nehls et al.
7,142,922	B2		11/2006	Spinelli et al.
7,184,835	B2		2/2007	Kramer et al.
7,215,998	B2		5/2007	Wesselink et al.
7,286,866	B2		10/2007	Okerlund et al.
7,308,297	B2		12/2007	Reddy et al.
7,308,299	B2		12/2007	Burrell et al.
7,313,444	B2		12/2007	Pianca et al.
7,321,677	B2		1/2008	Evron et al.
7,346,381	B2		3/2008	Okerlund et al.
7,398,116	B2		7/2008	Edwards
7,426,412	B1		9/2008	Schecter
7,454,248	B2		11/2008	Burrell et al.
7,499,743	B2		3/2009	Vass et al.
7,509,170	B2		3/2009	Zhang et al.
7,565,190	B2		7/2009	Okerlund et al.
7,587,074	B2		9/2009	Zarkh et al.
7,599,730	B2		10/2009	Hunter et al.
7,610,088	B2		10/2009	Chinchoy
7,613,500	B2		11/2009	Vass et al.
7,616,993	B2		11/2009	Müssig et al.
7,664,550	B2		2/2010	Eick et al.
7,684,863	B2		3/2010	Parikh et al.
7,742,629	B2		6/2010	Zarkh et al.
7,747,047	B2		6/2010	Okerlund et al.
7,751,882	B1		7/2010	Helland
7,769,451	B2		8/2010	Yang et al.
7,778,685	B2		8/2010	Evron et al.
7,778,686	B2		8/2010	Vass et al.
7,787,951	B1		8/2010	Min
7,813,785	B2		10/2010	Okerlund et al.
7,818,040	B2		10/2010	Spear et al.
7,848,807	B2		12/2010	Wang
7,860,580	B2		12/2010	Falk et al.
7,894,889	B2		2/2011	Zhang
7,912,544	B1		3/2011	Min et al.
7,917,214	B1		3/2011	Gill et al.
7,941,213	B2		5/2011	Markowitz et al.
7,953,475	B2		5/2011	Harlev et al.
7,953,482	B2		5/2011	Hess
7,983,743	B2		7/2011	Rudy et al.
7,996,063	B2		8/2011	Vass et al.
8,010,194	B2		8/2011	Muller
8,019,402	B1		9/2011	Kryzpow et al.
8,019,409	B2		9/2011	Rosenberg et al.
8,032,229	B2		10/2011	Gerber et al.
8,036,743	B2		10/2011	Savage et al.
8,060,185	B2		11/2011	Hunter et al.
8,150,513	B2		4/2012	Chinchoy
8,160,700	B1		4/2012	Ryu et al.
8,175,703	B2		5/2012	Dong et al.
8,180,428	B2		5/2012	Kaiser et al.
8,195,292	B2		6/2012	Rosenberg et al.
8,213,693	B1		7/2012	Li
8,214,041	B2		7/2012	Van Gelder et al.
8,265,738	B1		9/2012	Min et al.
8,285,377	B2		10/2012	Rosenberg et al.
8,295,943	B2		10/2012	Eggen et al.
8,326,419	B2		12/2012	Rosenberg et al.
8,332,030	B2		12/2012	Hess et al.

(56) **References Cited**

U.S. PATENT DOCUMENTS

8,380,308 B2 2/2013 Rosenberg et al.
8,401,616 B2 3/2013 Verard et al.
8,478,388 B2 7/2013 Nguyen et al.
8,527,051 B1 9/2013 Hedberg et al.
8,583,230 B2 11/2013 Ryu et al.
8,615,298 B2 12/2013 Ghosh et al.
8,617,082 B2 12/2013 Zhang et al.
8,620,433 B2 12/2013 Ghosh et al.
8,639,333 B2 1/2014 Stadler et al.
8,694,099 B2 4/2014 Ghosh et al.
8,738,132 B1 5/2014 Ghosh et al.
8,744,576 B2 6/2014 Munsterman et al.
8,768,465 B2 7/2014 Ghosh et al.
8,805,504 B2 8/2014 Sweeney
8,972,228 B2 3/2015 Ghosh
9,037,238 B2 5/2015 Stadler et al.
9,155,897 B2 10/2015 Ghosh et al.
9,199,087 B2 12/2015 Stadler et al.
9,265,951 B2 2/2016 Sweeney
9,265,954 B2 2/2016 Ghosh
9,265,955 B2 2/2016 Ghosh
9,278,219 B2 3/2016 Ghosh
9,278,220 B2 3/2016 Ghosh
9,282,907 B2 3/2016 Ghosh
2002/0087089 A1 7/2002 Ben-Haim
2002/0143264 A1 10/2002 Ding et al.
2002/0161307 A1 10/2002 Yu et al.
2002/0169484 A1 11/2002 Mathis et al.
2003/0018277 A1 1/2003 He
2003/0050670 A1 3/2003 Spinelli et al.
2003/0105495 A1 6/2003 Yu et al.
2003/0236466 A1 12/2003 Tarjan et al.
2004/0015081 A1 1/2004 Kramer et al.
2004/0059237 A1 3/2004 Narayan et al.
2004/0097806 A1 5/2004 Hunter et al.
2004/0102812 A1 5/2004 Yonce et al.
2004/0122479 A1 6/2004 Spinelli et al.
2004/0162496 A1 8/2004 Yu et al.
2004/0172078 A1 9/2004 Chinchoy
2004/0172079 A1 9/2004 Chinchoy
2004/0193223 A1 9/2004 Kramer et al.
2004/0215245 A1 10/2004 Stahmann et al.
2004/0215252 A1 10/2004 Verbeek et al.
2004/0220635 A1 11/2004 Burnes
2004/0267321 A1 12/2004 Boileau et al.
2005/0008210 A1 1/2005 Evron et al.
2005/0027320 A1 2/2005 Nehls et al.
2005/0090870 A1 4/2005 Hine et al.
2005/0096522 A1 5/2005 Reddy et al.
2005/0149138 A1 7/2005 Min et al.
2006/0074285 A1 4/2006 Zarkh et al.
2006/0224198 A1 10/2006 Dong et al.
2006/0235478 A1 10/2006 Van Gelder et al.
2006/0253162 A1 11/2006 Zhang et al.
2007/0142871 A1 6/2007 Libbus et al.
2007/0232943 A1 10/2007 Harel et al.
2007/0250129 A1 10/2007 Van Oort
2007/0265508 A1 11/2007 Sheikhzadeh-Nadjar et al.
2008/0021336 A1 1/2008 Dobak et al.
2008/0058656 A1 3/2008 Costello et al.
2008/0119903 A1 5/2008 Arcot-Krishnamurthy et al.
2008/0140143 A1 6/2008 Ettori et al.
2008/0146954 A1 6/2008 Bojovic et al.
2008/0242976 A1 10/2008 Robertson et al.
2008/0269818 A1 10/2008 Sullivan et al.
2008/0269823 A1 10/2008 Burnes et al.
2008/0281195 A1 11/2008 Heimdal
2008/0306567 A1 12/2008 Park et al.
2008/0306568 A1 12/2008 Ding et al.
2009/0005832 A1 1/2009 Zhu et al.
2009/0036947 A1 2/2009 Westlund et al.
2009/0043352 A1 2/2009 Brooke et al.
2009/0048528 A1 2/2009 Hopenfeld et al.
2009/0053102 A2 2/2009 Rudy et al.
2009/0054941 A1 2/2009 Eggen et al.
2009/0054946 A1 2/2009 Sommer et al.
2009/0084382 A1 4/2009 Jalde et al.
2009/0093857 A1 4/2009 Markowitz et al.
2009/0099468 A1 4/2009 Thiagalingam et al.
2009/0099469 A1 4/2009 Flores
2009/0099619 A1 4/2009 Lessmeier et al.
2009/0112109 A1 4/2009 Kuklik et al.
2009/0143838 A1 6/2009 Libbus et al.
2009/0157134 A1 6/2009 Ziglio et al.
2009/0157136 A1 6/2009 Yang et al.
2009/0198298 A1 8/2009 Kaiser et al.
2009/0216112 A1 8/2009 Assis et al.
2009/0232448 A1 9/2009 Barmash et al.
2009/0234414 A1 9/2009 Sambelashvili et al.
2009/0254140 A1 10/2009 Rosenberg et al.
2009/0270729 A1 10/2009 Corbucci et al.
2009/0270937 A1 10/2009 Yonce et al.
2009/0299201 A1 12/2009 Gunderson
2009/0299423 A1 12/2009 Min
2009/0306732 A1 12/2009 Rosenberg et al.
2009/0318995 A1 12/2009 Keel et al.
2010/0022873 A1 1/2010 Hunter et al.
2010/0049063 A1 2/2010 Dobak, III
2010/0069987 A1 3/2010 Min et al.
2010/0087888 A1 4/2010 Maskara
2010/0094149 A1 4/2010 Kohut et al.
2010/0113954 A1 5/2010 Zhou
2010/0114229 A1 5/2010 Chinchoy
2010/0121403 A1 5/2010 Schecter et al.
2010/0145405 A1 6/2010 Min et al.
2010/0174137 A1 7/2010 Shim
2010/0198292 A1 8/2010 Honeck et al.
2010/0228138 A1 9/2010 Chen
2010/0234916 A1 9/2010 Turcott et al.
2010/0254583 A1 10/2010 Chan et al.
2010/0268059 A1 10/2010 Ryu et al.
2011/0004111 A1 1/2011 Gill et al.
2011/0004264 A1 1/2011 Siejko et al.
2011/0022112 A1 1/2011 Min
2011/0054286 A1 3/2011 Crosby
2011/0054559 A1 3/2011 Rosenberg et al.
2011/0054560 A1 3/2011 Rosenberg et al.
2011/0075896 A1 3/2011 Matsumoto
2011/0092809 A1 4/2011 Nguyen et al.
2011/0112398 A1 5/2011 Zarkh et al.
2011/0118803 A1 5/2011 Hou et al.
2011/0137369 A1 6/2011 Ryu et al.
2011/0144510 A1 6/2011 Ryu et al.
2011/0172728 A1 7/2011 Wang
2011/0190615 A1 8/2011 Phillips et al.
2011/0201915 A1 8/2011 Gogin et al.
2011/0213260 A1 9/2011 Keel et al.
2011/0319954 A1 12/2011 Niazi et al.
2012/0004567 A1 1/2012 Eberle et al.
2012/0101543 A1 4/2012 Demmer et al.
2012/0101546 A1 4/2012 Stadler et al.
2012/0203090 A1 8/2012 Min
2012/0253419 A1 10/2012 Rosenberg et al.
2012/0283587 A1 11/2012 Ghosh et al.
2012/0284003 A1 11/2012 Ghosh et al.
2012/0296387 A1 11/2012 Zhang et al.
2012/0296388 A1 11/2012 Zhang et al.
2012/0302904 A1 11/2012 Lian et al.
2012/0303084 A1 11/2012 Kleckner et al.
2012/0310297 A1 12/2012 Sweeney
2012/0330179 A1 12/2012 Yuk et al.
2013/0006332 A1 1/2013 Sommer et al.
2013/0018250 A1 1/2013 Caprio et al.
2013/0018251 A1 1/2013 Caprio et al.
2013/0030491 A1 1/2013 Stadler et al.
2013/0060298 A1 3/2013 Splett et al.
2013/0072790 A1 3/2013 Ludwig et al.
2013/0096446 A1 4/2013 Michael et al.
2013/0116739 A1 5/2013 Brada et al.
2013/0131529 A1 5/2013 Jia et al.
2013/0131749 A1 5/2013 Sheldon et al.
2013/0131751 A1 5/2013 Stadler et al.
2013/0136035 A1 5/2013 Bange et al.
2013/0165983 A1 6/2013 Ghosh et al.

(56) **References Cited**

U.S. PATENT DOCUMENTS

2013/0165988	A1	6/2013	Ghosh
2013/0261471	A1	10/2013	Saha et al.
2013/0261688	A1	10/2013	Dong et al.
2013/0289640	A1	10/2013	Zhang et al.
2013/0296726	A1	11/2013	Niebauer et al.
2013/0304407	A1	11/2013	George et al.
2013/0324828	A1	12/2013	Nishiwaki et al.
2014/0005563	A1	1/2014	Ramanathan et al.
2014/0018872	A1	1/2014	Siejko et al.
2014/0135866	A1	5/2014	Ramanathan et al.
2014/0135867	A1	5/2014	Demmer et al.
2014/0222099	A1	8/2014	Sweeney
2014/0236252	A1	8/2014	Ghosh et al.
2014/0323882	A1	10/2014	Ghosh et al.
2014/0323892	A1	10/2014	Ghosh et al.
2014/0323893	A1	10/2014	Ghosh et al.
2014/0371807	A1	12/2014	Ghosh et al.
2014/0371808	A1	12/2014	Ghosh et al.
2014/0371832	A1	12/2014	Ghosh et al.
2014/0371833	A1	12/2014	Ghosh et al.
2015/0032016	A1	1/2015	Ghosh
2015/0032172	A1	1/2015	Ghosh
2015/0032173	A1	1/2015	Ghosh
2015/0045849	A1	2/2015	Ghosh et al.
2015/0142069	A1	5/2015	Sambelashvili
2015/0157225	A1	6/2015	Gillberg et al.
2015/0157231	A1	6/2015	Gillberg et al.
2015/0157232	A1	6/2015	Gillberg et al.
2015/0157865	A1	6/2015	Gillberg et al.
2015/0265840	A1	9/2015	Ghosh et al.
2016/0030751	A1	2/2016	Ghosh et al.

FOREIGN PATENT DOCUMENTS

CN	1878595	12/2006
CN	101073502	11/2007
EP	1 072 284 A2	1/2001
EP	1 504 713 A1	2/2005
EP	2 016 976 A1	1/2009
EP	1 925 337 B1	3/2012
EP	2 436 309 A2	4/2012
EP	2 435 132 B1	8/2013
WO	WO 98/26712 A1	6/1998
WO	WO 99/06112 A1	2/1999
WO	WO 00/45700 A1	8/2000
WO	WO 01/67950 A1	9/2001
WO	03070323 A1	8/2003
WO	WO 2005/056108 A2	6/2005
WO	2006069215 A2	6/2006
WO	WO 2006/105474 A2	10/2006
WO	WO 2006/115777 A1	11/2006
WO	WO 2006/117773 A1	11/2006
WO	WO 2007/013994 A2	2/2007
WO	2007027940 A2	3/2007
WO	WO 2007/013994 A3	4/2007
WO	WO 2007/139456 A1	12/2007
WO	WO 2008/151077 A2	12/2008
WO	WO 2009/079344 A1	6/2009
WO	WO 2009/139911 A2	11/2009
WO	WO 2009/148429 A1	12/2009
WO	WO 2010/019494 A1	2/2010
WO	WO 2010/071520 A1	6/2010
WO	WO 2010/088040 A1	8/2010
WO	WO 2010/088485 A1	8/2010
WO	WO 2011/070166 A1	6/2011
WO	WO 2011/090622 A1	7/2011
WO	WO 2011/099992 A1	8/2011
WO	WO 2012/037471 A2	3/2012
WO	WO 2012/037471 A3	6/2012
WO	WO 2012/106297 A2	8/2012
WO	WO 2012/106297 A3	8/2012
WO	WO 2012/109618 A2	8/2012
WO	WO 2012/110940 A1	8/2012
WO	WO 2012/109618 A3	11/2012
WO	WO 2012/151364 A1	11/2012
WO	WO 2012/151389 A1	11/2012
WO	WO 2013/006724 A2	1/2013
WO	WO 2013/010165 A1	1/2013
WO	WO 2013/010184 A1	1/2013
WO	WO 2013/006724 A3	4/2013
WO	WO 2014/179454 A1	11/2014
WO	WO 2014/179459 A2	11/2014
WO	WO 2014/179459 A3	1/2015
WO	WO 2015/013271 A1	1/2015
WO	WO 2015/013493 A1	1/2015
WO	WO 2015013574 A1	1/2015

OTHER PUBLICATIONS

(PCT/US2012/036262) PCT Notification of Transmittal of the International Search Report and the Written Opinion of the International Searching Authority.

"Accuracy of Quadratic Versus Linear Interpolation in Noninvasive Electrocardiographic Imaging (ECGI)", by Subham Ghosh and Yoram Rudy, *Annuals of Biomedical Engineering*, vol. 33, No. 9, Sep. 2005, pp. 1187-1201.

"Method of Segmentation of Thorax Organs Images Applied to Modelling the Cardiac Electrical Field", by Alina Czerwinska et al., Engineering in Medicine and Biology Society, *Proceedings of the22nd Annual International Conference of the IEEE*, vol. 1, Jul. 23, 2000, pp. 402-405.

"The Forward and Inverse Problems of Electrocardiography", by Ramesh M. Gulrajani, *IEEE Engineering in Medicine and Biology*, IEEE Service Center, vol. 17, No. 5, Sep. 1, 1988, pp. 84-101, 122.

"Cardiac resynchronization therapy in pediatric congenital heart disease: Insights from noninvasive electrocardiographic imaging", by Jennifer N.A. Silva, M.D., et al., *Heart Rhythm*, vol. 6, No. 8, Aug. 1, 2009, pp. 1178-1185.

"Electrocardiographic imaging of cardiac resynchronization therapy in heart failure: Observation of variable electrophysiologic responses", by Ping Jia, Ph.D. et al., *Heart Rhythm*, vol. 3, No. 3, Mar. 1, 2006, pp. 296-310.

Ghosh et al., "Accuracy of Quadratic Versus Linear Interpolation in Non-Invasive Electrocardiographic Imaging (ECGI)," Annals of Biomedical Engineering, vol. 33, No. 9, Sep. 2005, pp. 1187-1201.

Ghosh et al., "Application of the L1-Norm Regularization to Epicardial Potential Solution of the Inverse Electrocardiography Problem," Annals of Biomedical Engineering, vol. 37, No. 5, 2009, 11 pp.

Modre et al., "Noninvasive Myocardial Activation Time Imaging: A Novel Inverse Algorithm Applied to Clinical ECG Mapping Data," IEEE Transactions on Biomedical Engineering, vol. 49, No. 10, Oct. 2002, pp. 1153-1161.

Williams et al., "Short-term hemodynamic effects of cardiac resynchronization therapy in patients with heart failure, a narrow QRS duration and no dyssynchrony," Circulation 2009;120:1687-1694.

Turner et al., "Electrical and mechanical components of dyssynchrony in heart failure patients with normal QRS duration and left bundle-branch block," Circulation 2004; 109:2544-2549.

Kornreich, "Body surface potential mapping of ST segment changes in acute myocardial infarction," Circulation 1993; 87:773-782.

Varma et al., "Placebo CRT," J Cardiovasc Electrophysiol, vol. 19, p. 878, Aug. 2008.

Miri et al., "Applicability of body surface potential map in computerized optimization of biventricular pacing," Annals of Biomedical Engineering, vol. 38(3), Mar. 2010, pp. 865-875.

Miri et al., "Comparison of the electrophysiologically based optimization methods with different pacing parameters in patient undergoing resynchronization treatment," 30th Annual International IEEE EMBS Conference, Aug. 2008, pp. 1741-1744.

Miri et al., "Computerized Optimization of Biventricular Pacing Using Body Surface Potential Map," 31st Annual International Conference of the IEEE EMBS, Sep. 2009, pp. 2815-2818.

Miri et al., "Efficiency of Timing Delays and Electrode Positions in Optimization of Biventricular Pacing: A Simulation Study," IEEE Transactions on Biomedical Engineering, vol. 56(11), Nov. 2009, pp. 2573-2582.

(56) **References Cited**

OTHER PUBLICATIONS

Svendsen et al., "Computational Models of Cardiac Electrical Activation," Computational Cardiovascular Mechanics, Chapter 5, 2010, pp. 73-88.

Wang et al., "Application of the Method of Fundamental Solutions to Potential-based Inverse Electrocardiography," Annals of Biomedical Engineering, vol. 34(8), Aug. 2006, pp. 1272-1288.

Prosecution History from U.S. Appl. No. 13/462,480, dated Jul. 3, 2014 through Oct. 22, 2014, 39 pp.

First Office Action and Search Report, and translation thereof, from counterpart Chinese Application No. 201280024669.3, dated Dec. 16, 2014, 18 pp.

Biffi et al., "Occurrence of Phrenic Nerve Stimulation in Cardiac Resynchronization Therapy Patients: The Role of Left Ventricular Lead Type and Placement Site," *Europace*, Jul. 29, 2012, 15:77-82.

Botker MD, PhD., et al., "Electromechanical Mapping for Detection of Myocardial Viability in Patients with ischemia Cardiomyopathy," Circulation, Mar. 2001; vol. 103, No. 12, pp. 1631-1637.

"CardioGuide System Enables Real-Time Navigation of Left Ventricular Leads During Medtronic CRT Implants," Press Release, Apr. 9, 2013, Medtronic, Inc., 2 pgs.

Cuculich, P.S., et al., "The Electrophysiological Cardiac Ventricular Substrate in Patients After Myocardial Infection" J. Am. Coll. Cardiol. Nov. 28, 2011; 58:1893-1902.

Dawoud, F. et al., "Inverse Electrocardiographic Imaging to Assess Electrical Dyssynchrony in Cardiac Resynchronization Therapy Patients," Computing in Cardiology, Sep. 2012; 39:993-996.

Freund et al., "A Decision-Theoretic Generalization of On-line Learning and an Application to Boosting," Journal of Computer and System Sciences, Dec. 1996; 55(1):119-139.

Friedman, "Greedy Function Approximation: A Gradient Boosting Machine," Annals of Statistics, Oct. 2001; 29(5):1189-1232.

Friedman, "Stochastic Gradient Boosting," Computational Statistics and Data Analysis, Feb. 2002; 38(4):337-374.

Friedman et al., "Additive Logistic Regression: a Statistical View of Boosting," Annals of Statistics, Apr. 2000; 28(2):337-374.

Ghosh et al., "Cardiac Memory in Patents with Wolff-Parkinson-White Syndrome: Noninvasive Imaging of Activation and Repolarization Before and After Catheter Ablation," Circulation, Aug. 12, 2008; 118:907-915.

Ghosh et al., "Electrophysiological Substrate and Intraventricular LV Dyssynchrony in Non-ischemic Heart Failure Patients Undergoing Cardiac Resynchronization Therapy," Heart rhythm: the official journal of the Heart Rhythm Society, Jan. 2011; 8(5):692-699.

Gold et al., "Comparison of Stimulation Sites within Left Ventricular Veins on the Acute Hemodynatnic Effects of Cardiac Resynchronization Therapy," Heart Rhythm, Apr. 2005; 2(4):376-381.

Hansen, "Regularization Tools: A Matlab Package for Analysis and Solution of Discrete Ill-Posed Problems," Version 4.1 for Matlab 7.3; Mar. 2008; 128 pages. Retrieved from the Internet: Jun. 19, 2014 http://www.mathworks.com/matlabcentral/fileexchange/52-regtools.

Hayes et al., "Cardiac Resynchronization Therapy and the Relationship of Percent Biventricular Pacing to Symptoms and Survival," Heart Rhythm, Sep. 2011; 8(9):1469-1475.

"Heart Failure Management" datasheet [online]. Medtronic, Minneapolis, Minnesota, [Last updated on Jun. 3, 2013]. Retrieved from the Internet: www.medtronic.com; 9 pages.

Hopenfeld et al., "The Effect of Conductivity on ST-Segment Epicardial Potentials Arising from Subendocardial Ischemia," Annals of Biomedical Eng., Jun. 2005; vol. 33, No. 6, pp. 751-763.

Medtronic Vitatron CARELINK ENCORE® Programmer Model 29901 Reference Manual, Jan. 29, 2013, 21 pp. Medtronic, Inc., Minneapolis, MN.

Nash et al., "An Experimental-Computational Framework for Validating in-vivo ECG Inverse Algorithms," International Journal of Bioelectromagnetism, vol. 2, No. 2, Dec. 31, 2000, 9 pp.

Potse et al., "Mathematical Modeling and Simulation of Ventricular Activation Sequences: Implications for Cardiac Resynchronization Therapy," J. of Cardiovasc. Trans. Res., Jan. 27, 2012; 5:146-158.

Prinzen et al., "Cardiac Resynchronization Therapy State-of-the-Art of Current Applications, Guidelines, Ongoing Trials, and Areas of Controversy", Circulation, Nov. 26, 2013; 128: 2407-2418.

Ridgeway, "The State of Boosting," Computing Science and Statistics, 1999; 31:172-181. (Applicant points out, in accordance with MPEP 609.04(a), that the year of publication, 1999, is sufficiently earlier than the effective U.S. filing date, May 2, 2012 so that the particular month of publication is not in issue.)

Ryu et al., "Simultaneous Electrical and Mechanical Mapping Using 3D Cardiac Mapping System: Novel Approach for Optimal Cardiac Resynchronization Therapy," Journal of Cardiovascular Electrophysiology, Feb. 2010; 21(2):219-22.

Singh et al., "Left Ventricular Lead Position and Clinical Outcome in the Multicenter Automatic Defibrillator Implantation Trial-Cardiac Resynchronization Therapy (MADIT-CRT) Trial," Circulation, Mar. 22, 2011; 123:1159-1166.

Sperzel et al., "Intraoperative Characterization of Interventricular Mechanical Dyssynchrony Using Electroanatomic Mapping System—a Feasibility Study," Journal of Interventional Cardiac Electrophysiology, Nov. 2012, 35(2):189-96.

Steinhaus BM., "Estimating cardiac transmembrane activation and recovery times from unipolar and bipolar extracellular electrograms: a simulation study," Circulation Research, Mar. 1989, 64:449-462.

Strik et al., "Electrical and Mechanical Ventricular Activation During Left Bundle Branch Block and Resynchronization," J. of Cardiovasc. Trans. Res., Feb. 7, 2012; 5:117-126.

Sweeney et al., "Analysis of Ventricular Activation Using Surface Electrocardiography to Predict Left Ventricular Reverse Volumetric Remoldeling During Cardiac Resynchronization Therapy," Circulation, Feb. 9, 2010; 121(5):626-34.

Van Deursen et al., "Vectorcardiography as a Tool for Wasy Optimization of Cardiac Resynchronization Therapy in Canine LBBB Hearts," Circulation Arrhythmia and Electrophysiology, Jun. 1, 2012; 5(3):544-52.

Vardas et al., The Task Force for Cardiac Pacing and Cardiac Resynchronization Therapy of the European Society of Cardiology. Developed in Collaboration with the European Heart Rhythm Association, European Heart Journal, Aug. 2007; 28:2256-2295.

Wellens, MD et al., "The Electrocardiogram 102 Years After Einthoven," Circulation, Feb. 2004; vol. 109, No. 5, pp. 562-564.

Ridgeway, "The State of Boosting," Computing Science and Statistics, 1999; 31:172-181. (Applicant points out, in accordance with MPEP 609.04(a), that the year of publication, 1999, is sufficiently earlier than the effective U.S. filing date, May 2, 2012 so that the particular month of publication is not in issue.).

Sperzel et al., "Intraoperative Characterization of Interventricular Mechanical Dyssynchrony Using Electroanatomic Mapping System—A Feasibility Study," Journal of Interventional Cardiac Electrophysiology, Nov. 2012; 35 (2):189-96.

Sweeney et al., "Analysis of Ventricular Activation Using Surface Electrocardiography to Predict Left Ventricular Reverse Volumetric Remoldeling During Cardiac Resynchronization Therapy," Circulation, Feb. 9, 2010; 121 (5):626-34.

Fung, et al., "Chapter 20, Optimization of Cardiac Resynchronization Therapy," Cardiac Resynchronization Therapy, Second Edition, Jan. 2009, pp. 356-373.

Sweeney, et al., "QRS Fusion Complex Analysis Using Wave Interference to Predict Reverse Remodeling During Cardiac Resynchronization Therapy," Heart Rhythm, May 2014, 11:806-813.

* cited by examiner

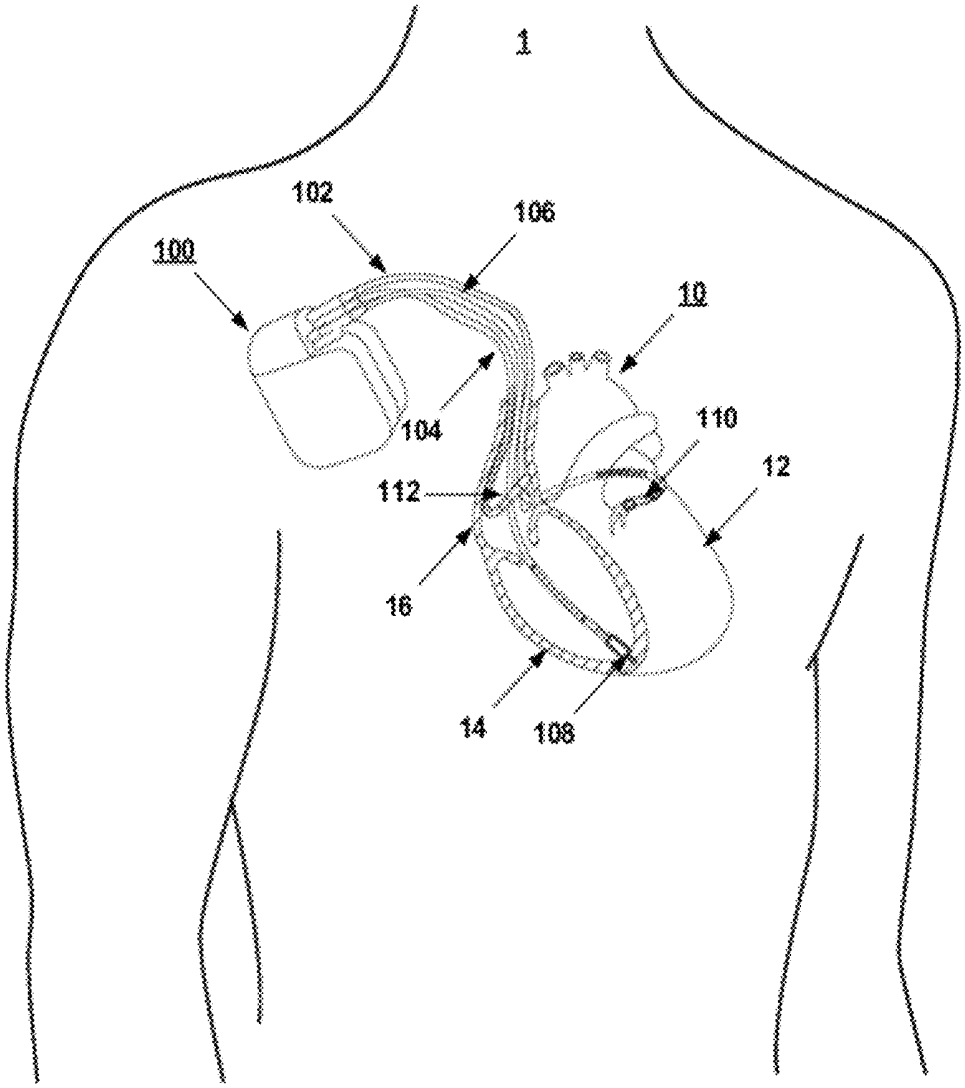

FIG. 1

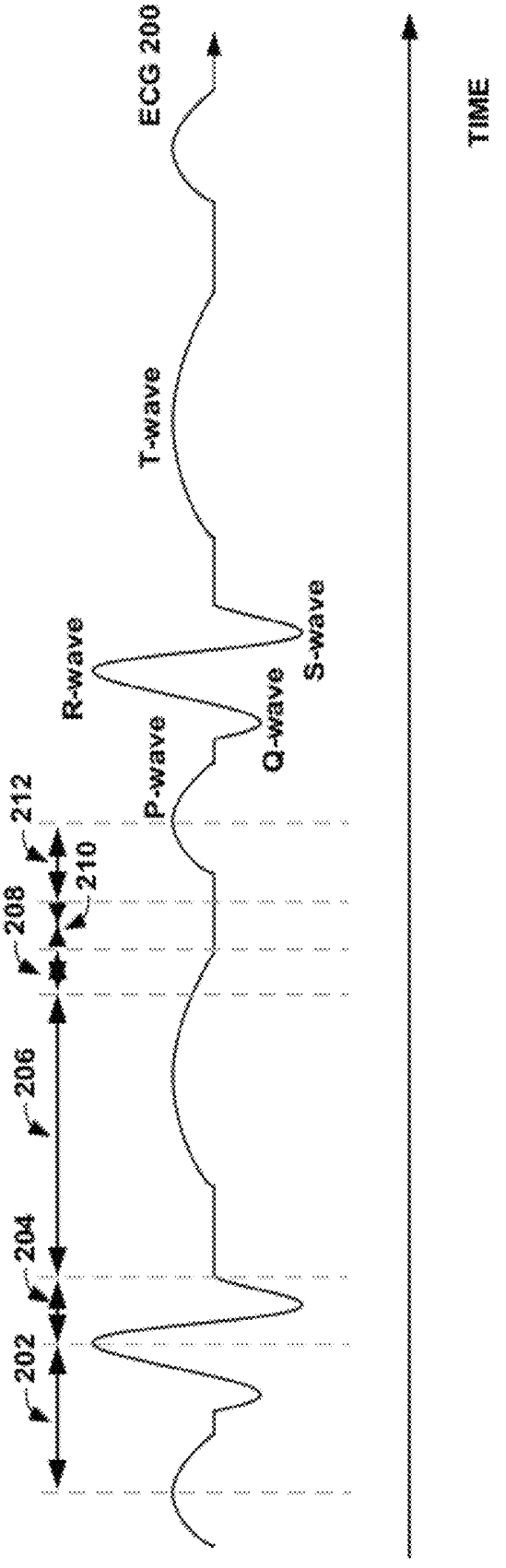
ECG 200
TIME
T-wave
S-wave
R-wave
Q-wave
P-wave
212
210
208
206
204
202

FIG. 2

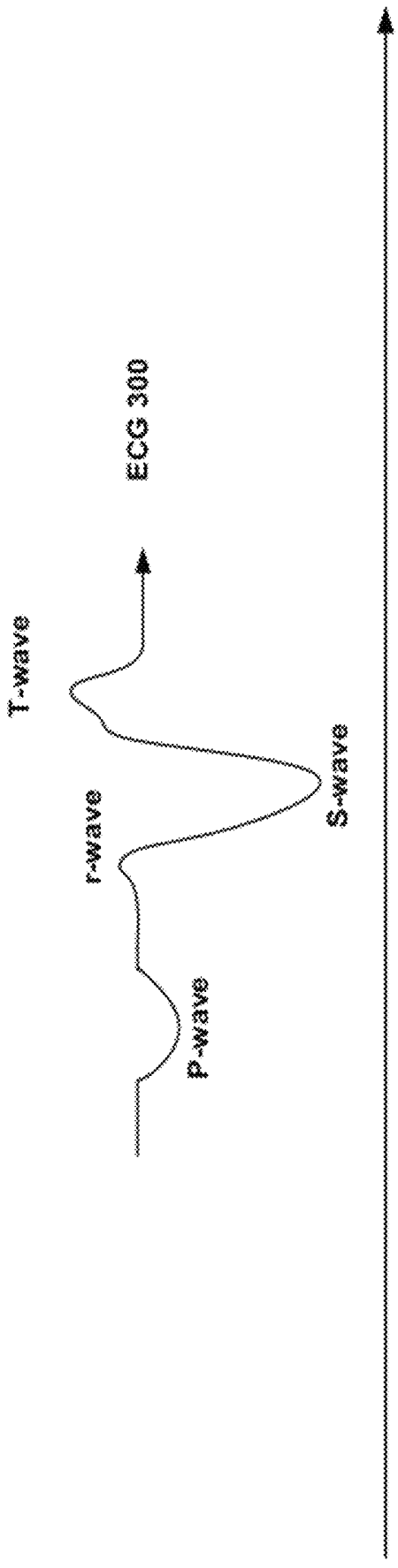

FIG. 3

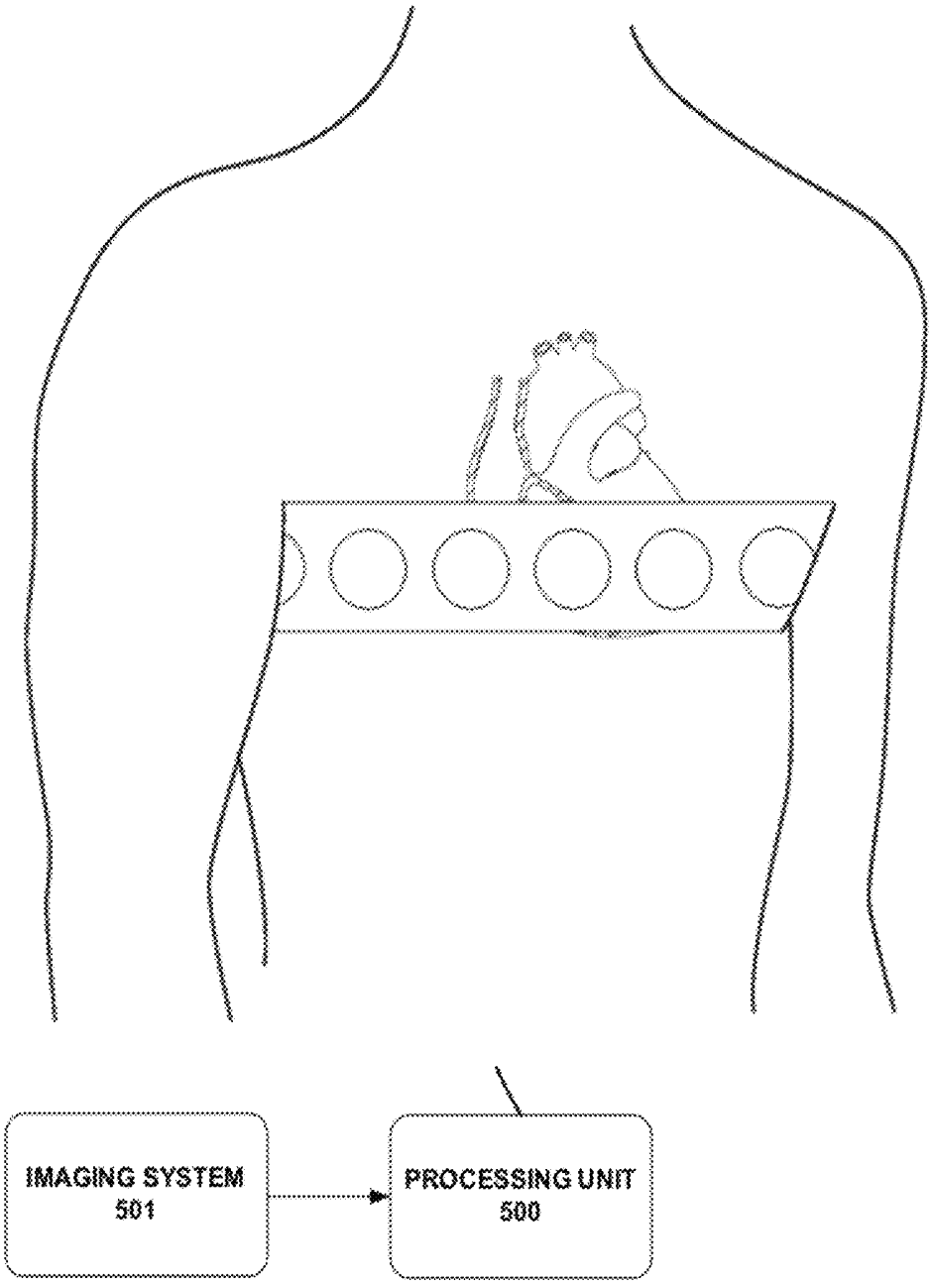

FIG. 4A

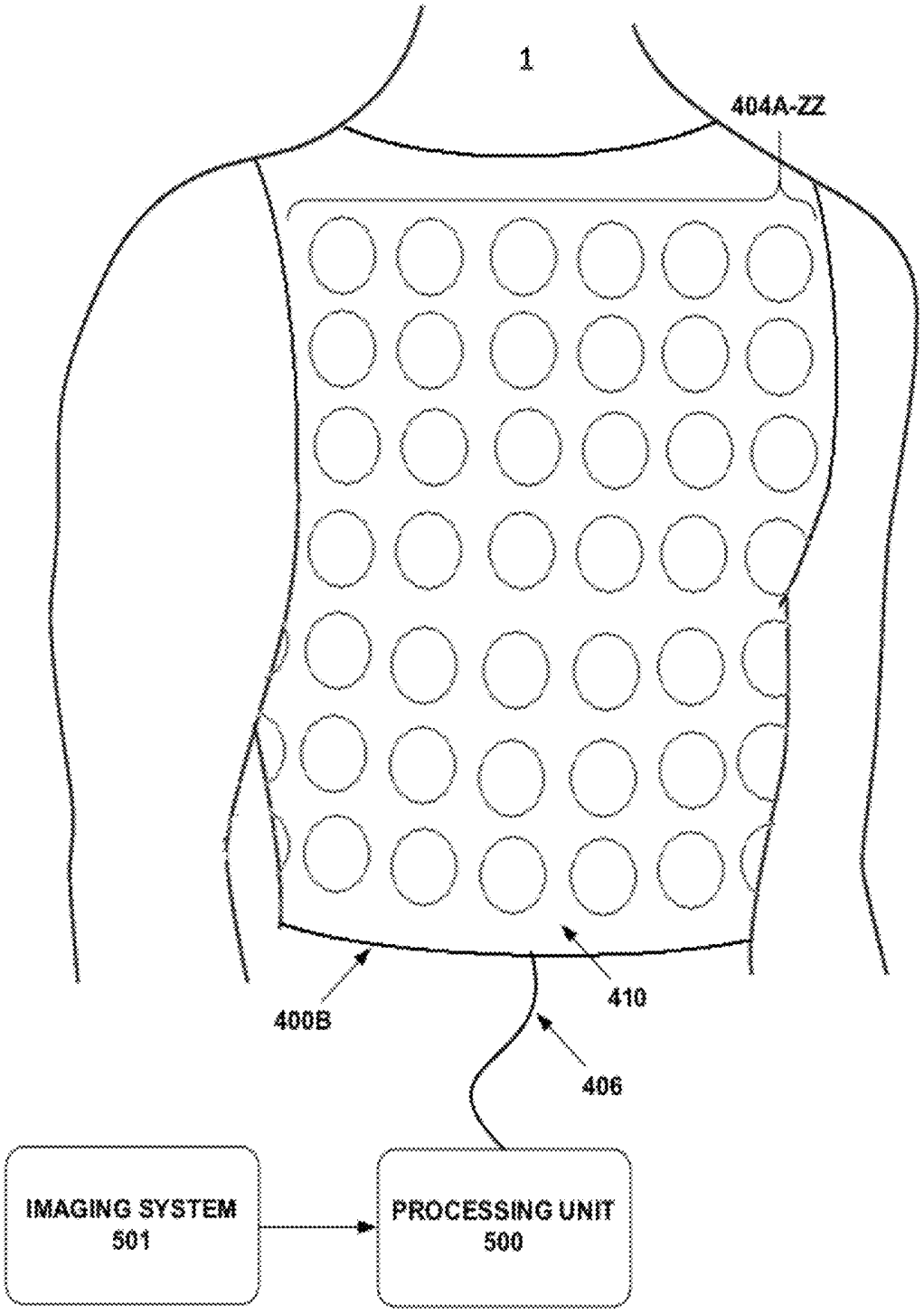
1
404A-ZZ
400B
410
406
IMAGING SYSTEM
501
PROCESSING UNIT
500

FIG. 4B

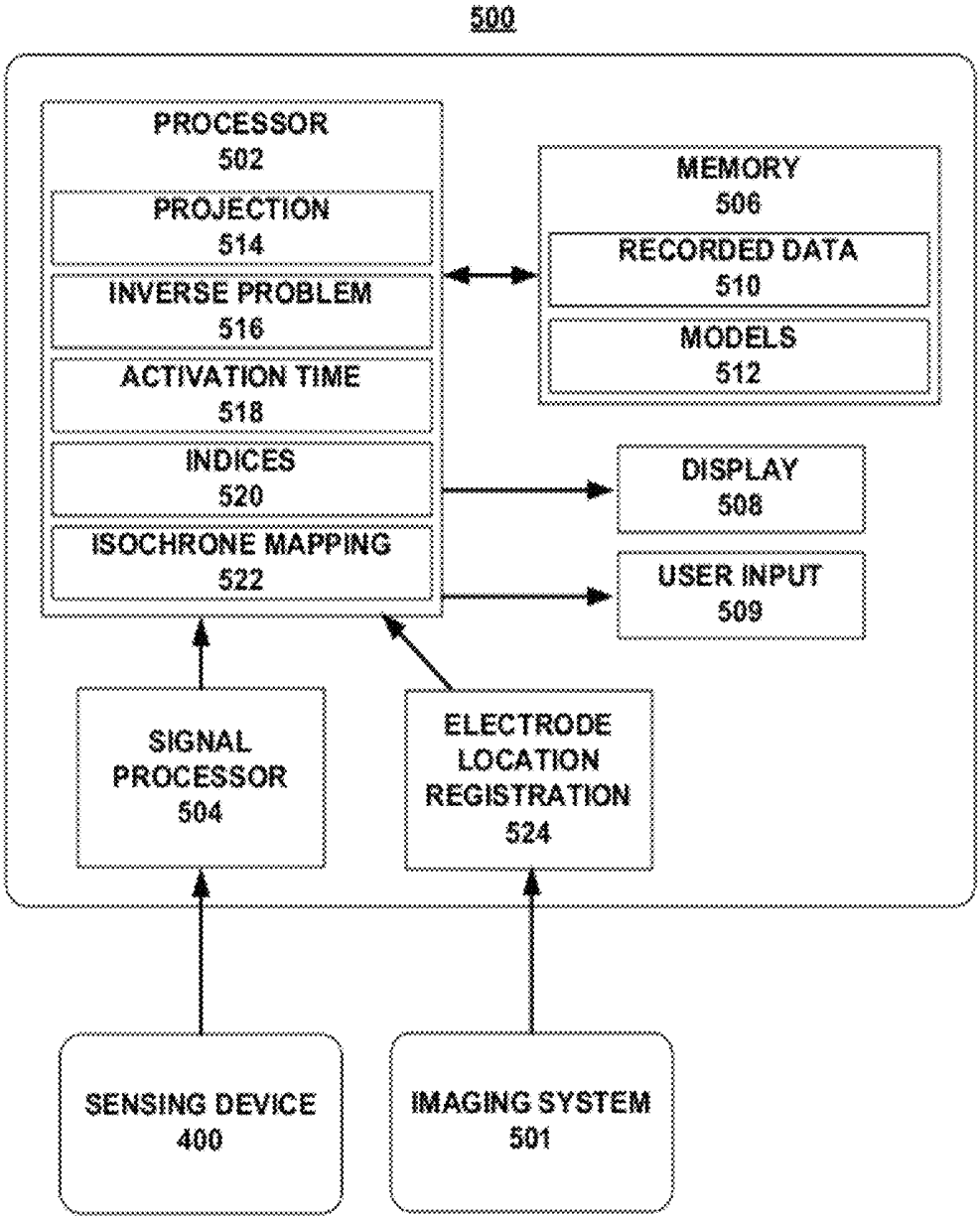
500
PROCESSOR
502
PROJECTION
514
INVERSE PROBLEM
516
ACTIVATION TIME
518
INDICES
520
ISOCHRONE MAPPING
522
MEMORY
506
RECORDED DATA
510
MODELS
512
DISPLAY
508
USER INPUT
509
SIGNAL
PROCESSOR
504
ELECTRODE
LOCATION
REGISTRATION
524
SENSING DEVICE
400
IMAGING SYSTEM
501

FIG. 5

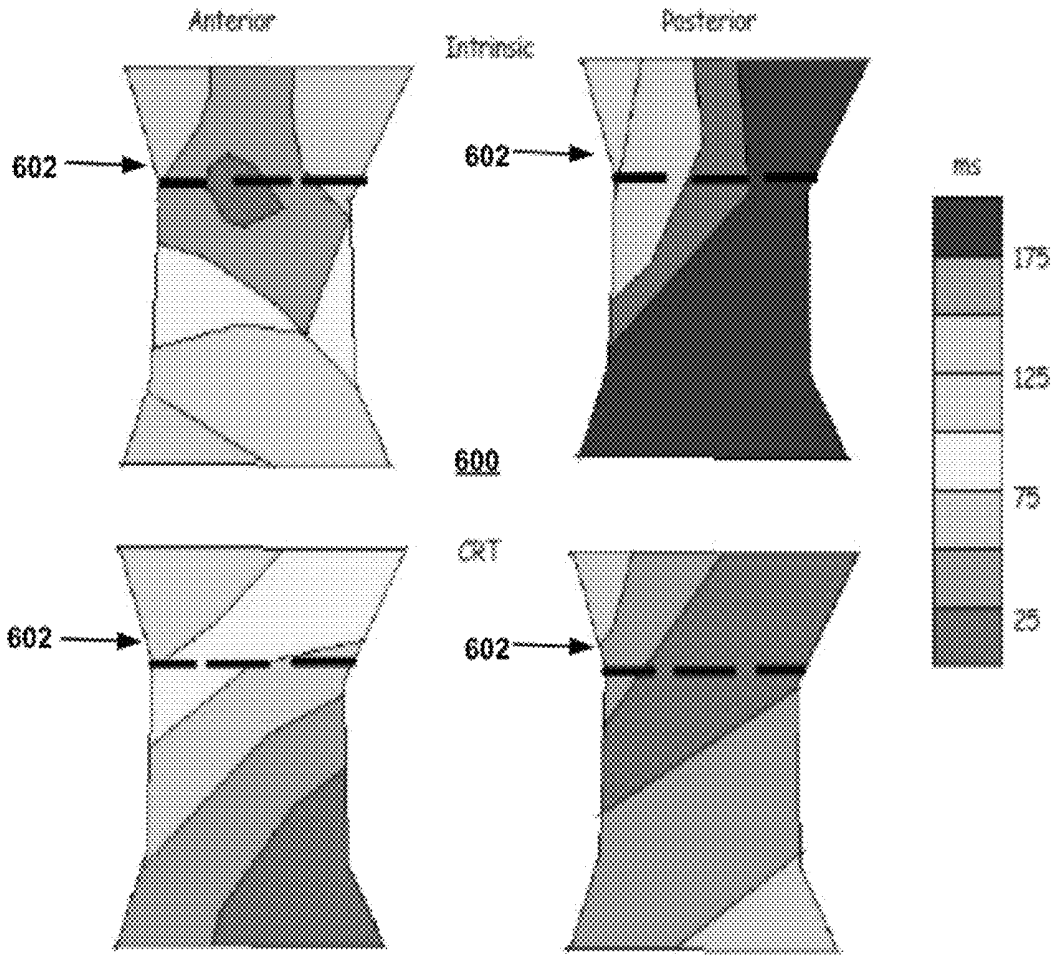
Anterior
Intrinsic
Posterior
602
602
ms
175
125
75
25
600
CRT
602
602

FIG. 6

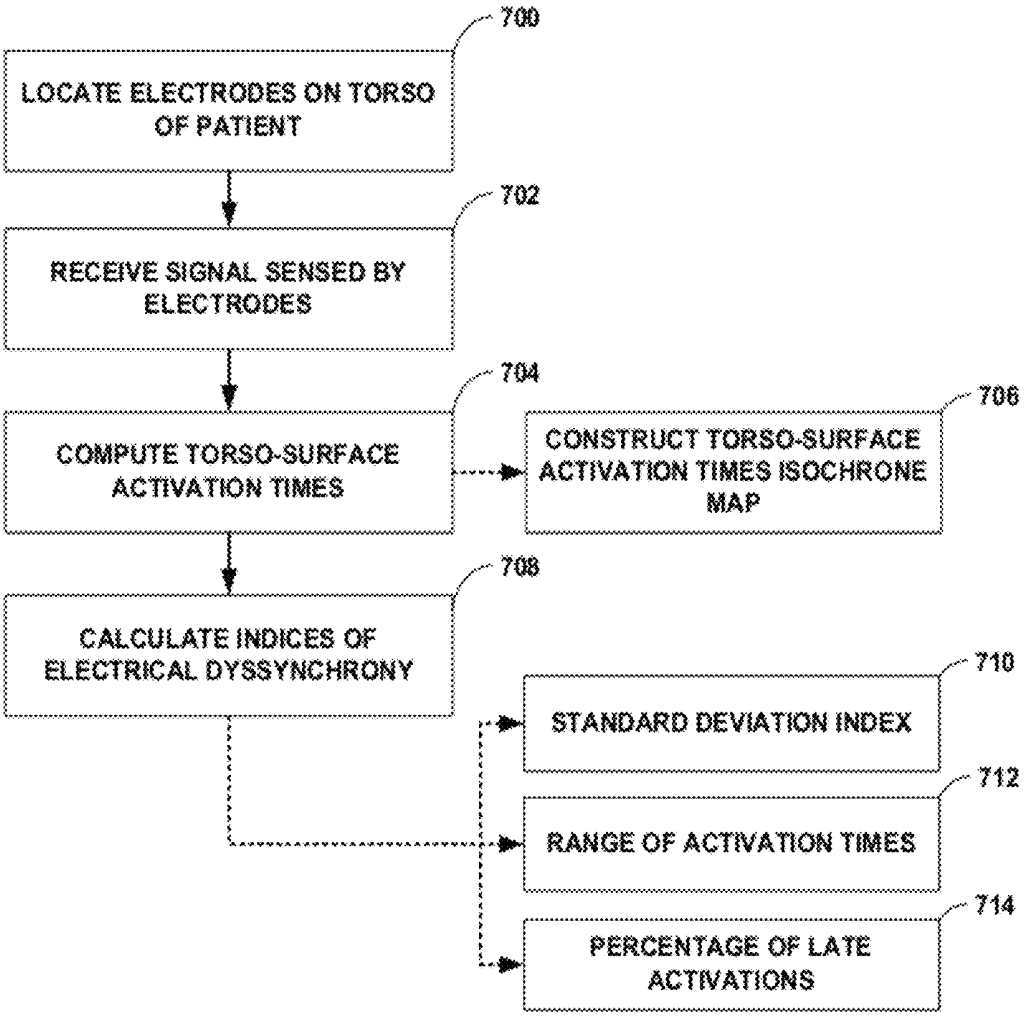
700
LOCATE ELECTRODES ON TORSO OF PATIENT
702
RECEIVE SIGNAL SENSED BY ELECTRODES
704
COMPUTE TORSO-SURFACE ACTIVATION TIMES
706
CONSTRUCT TORSO-SURFACE ACTIVATION TIMES ISOCHRONE MAP
708
CALCULATE INDICES OF ELECTRICAL DYSSYNCHRONY
710
STANDARD DEVIATION INDEX
712
RANGE OF ACTIVATION TIMES
714
PERCENTAGE OF LATE ACTIVATIONS

FIG. 7

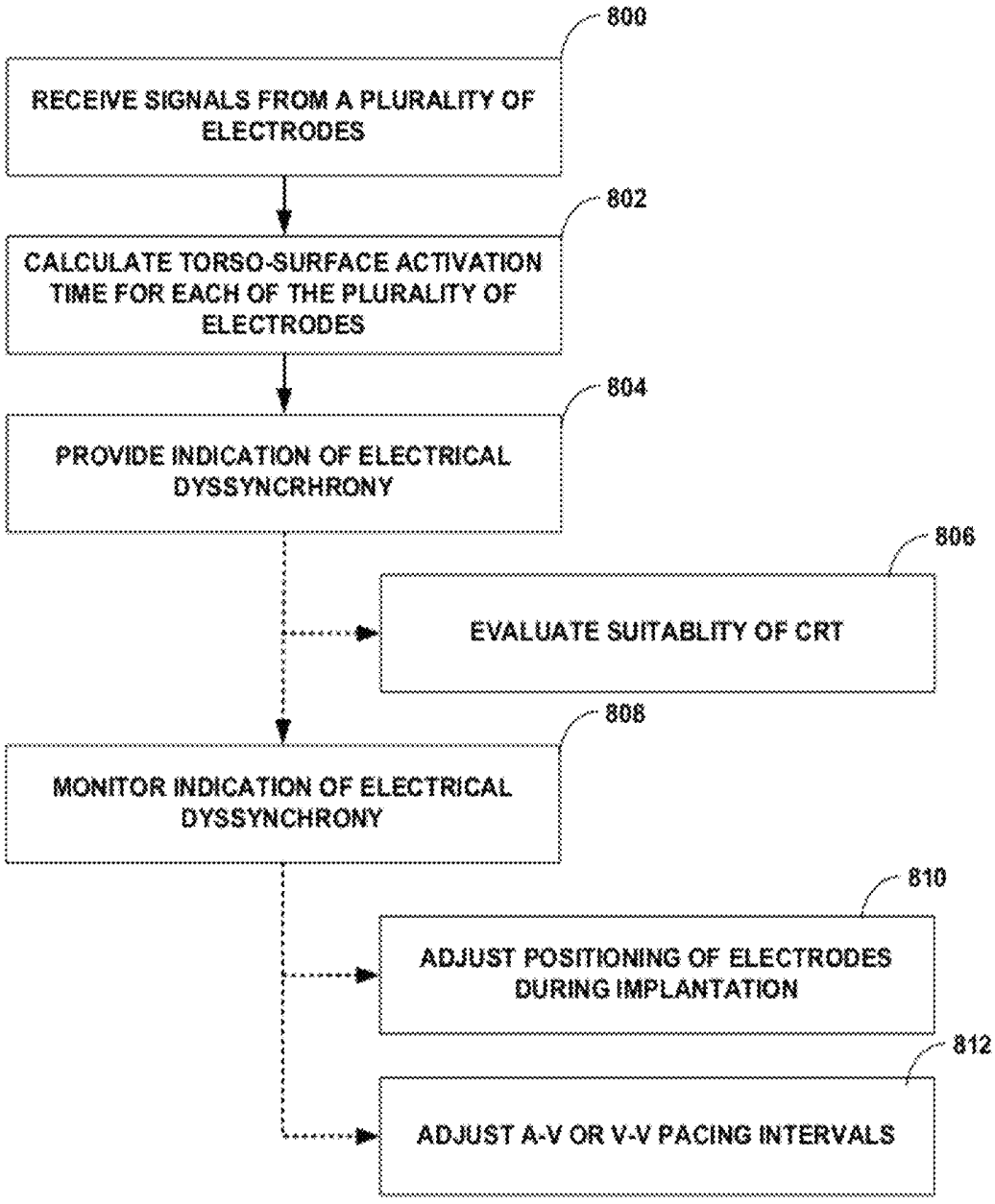
800
RECEIVE SIGNALS FROM A PLURALITY OF ELECTRODES
802
CALCULATE TORSO-SURFACE ACTIVATION TIME FOR EACH OF THE PLURALITY OF ELECTRODES
804
PROVIDE INDICATION OF ELECTRICAL DYSSYNCRHRONY
806
EVALUATE SUITABLITY OF CRT
808
MONITOR INDICATION OF ELECTRICAL DYSSYNCHRONY
810
ADJUST POSITIONING OF ELECTRODES DURING IMPLANTATION
812
ADJUST A-V OR V-V PACING INTERVALS

FIG. 8

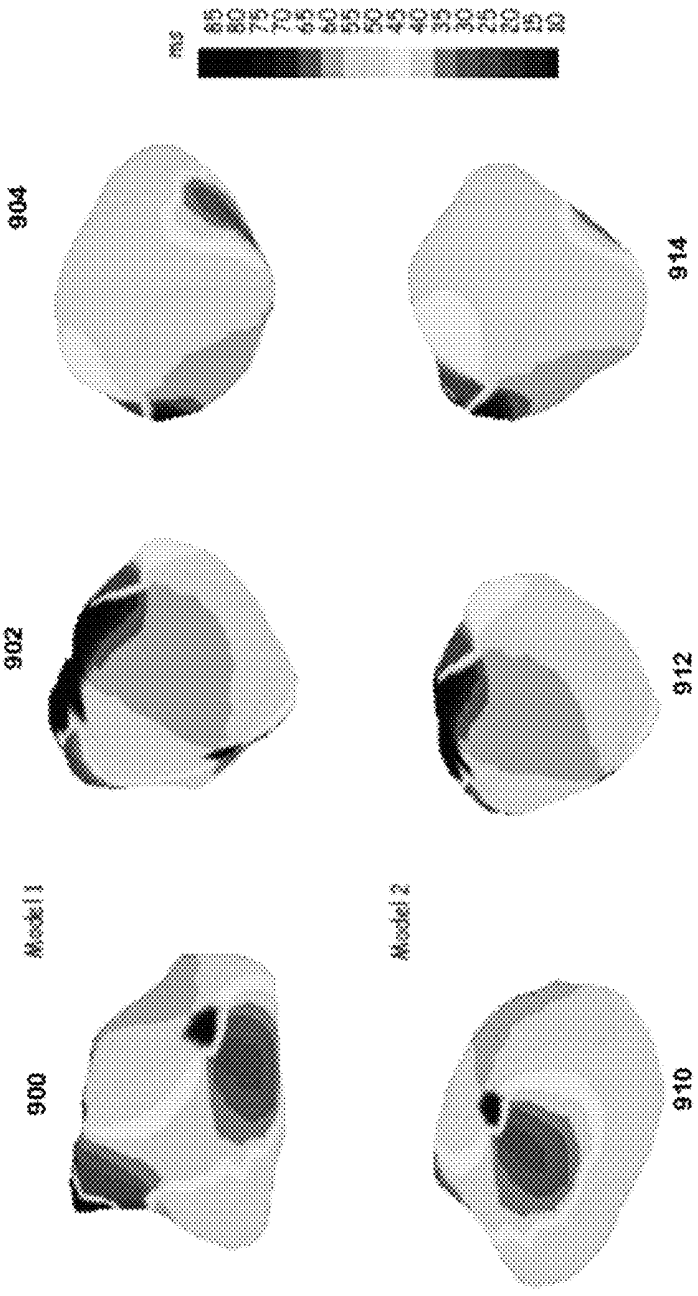

FIG. 9

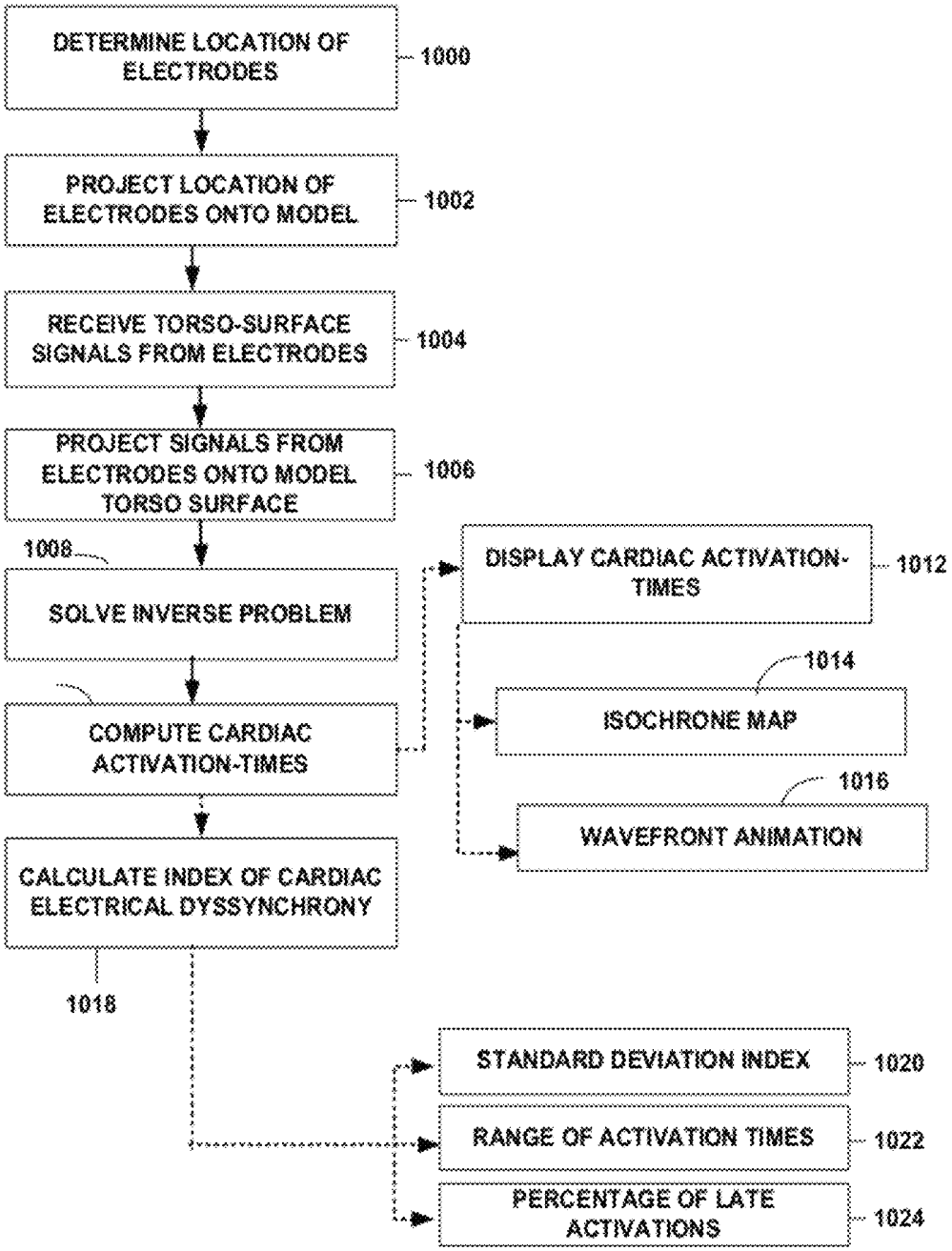
DETERMINE LOCATION OF ELECTRODES
1000
PROJECT LOCATION OF ELECTRODES ONTO MODEL
1002
RECEIVE TORSO-SURFACE SIGNALS FROM ELECTRODES
1004
PROJECT SIGNALS FROM ELECTRODES ONTO MODEL TORSO SURFACE
1006
1008
SOLVE INVERSE PROBLEM
COMPUTE CARDIAC ACTIVATION-TIMES
CALCULATE INDEX OF CARDIAC ELECTRICAL DYSSYNCHRONY
1018
DISPLAY CARDIAC ACTIVATION-TIMES
1012
1014
ISOCHRONE MAP
1016
WAVEFRONT ANIMATION
STANDARD DEVIATION INDEX
1020
RANGE OF ACTIVATION TIMES
1022
PERCENTAGE OF LATE ACTIVATIONS
1024

FIG. 10

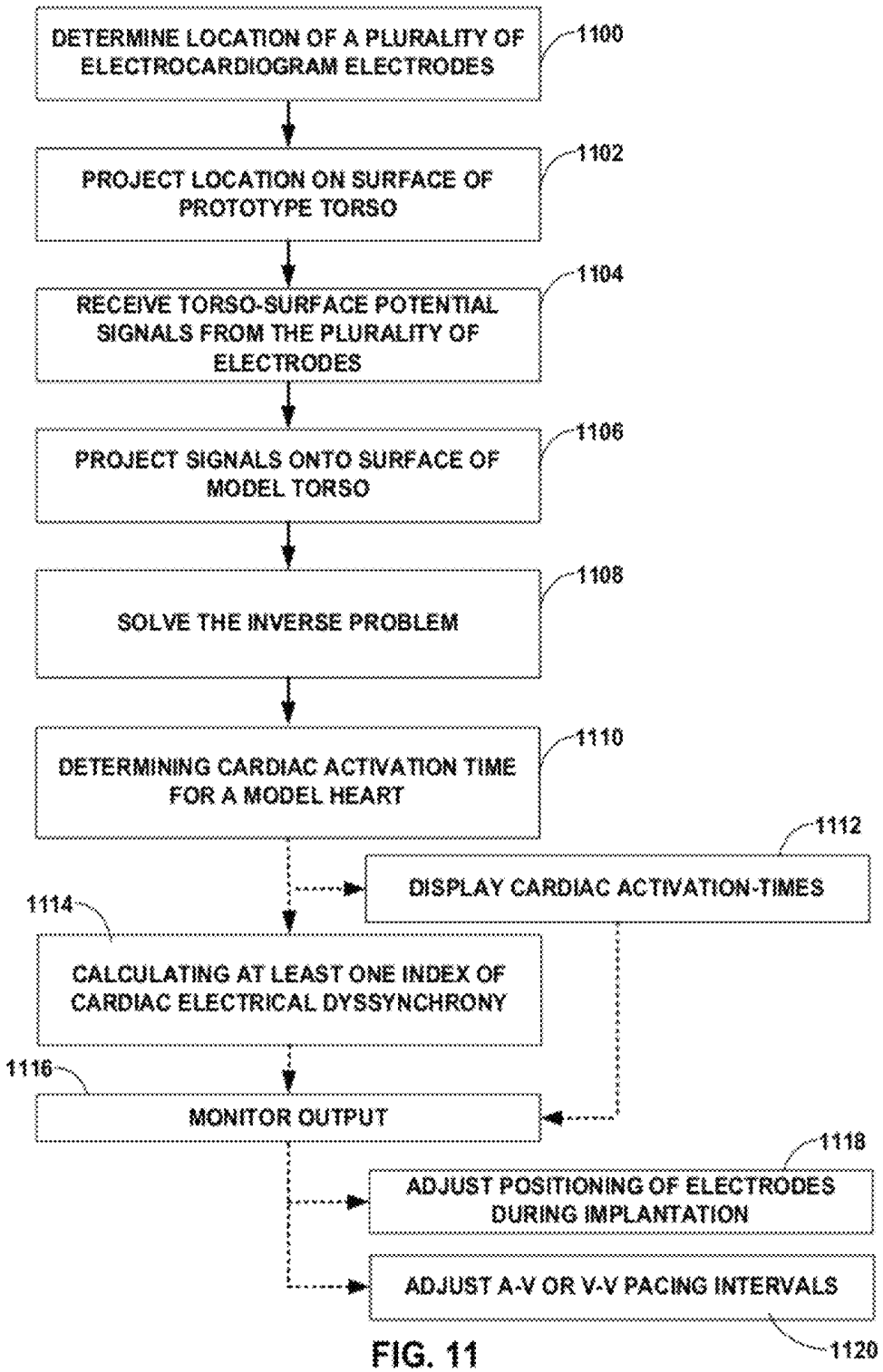
DETERMINE LOCATION OF A PLURALITY OF ELECTROCARDIOGRAM ELECTRODES
1100
PROJECT LOCATION ON SURFACE OF PROTOTYPE TORSO
1102
RECEIVE TORSO-SURFACE POTENTIAL SIGNALS FROM THE PLURALITY OF ELECTRODES
1104
PROJECT SIGNALS ONTO SURFACE OF MODEL TORSO
1106
SOLVE THE INVERSE PROBLEM
1108
DETERMINING CARDIAC ACTIVATION TIME FOR A MODEL HEART
1110
DISPLAY CARDIAC ACTIVATION-TIMES
1112
CALCULATING AT LEAST ONE INDEX OF CARDIAC ELECTRICAL DYSSYNCHRONY
1114
MONITOR OUTPUT
1116
ADJUST POSITIONING OF ELECTRODES DURING IMPLANTATION
1118
ADJUST A-V OR V-V PACING INTERVALS
1120

FIG. 11

ASSESSING INTRA-CARDIAC ACTIVATION PATTERNS AND ELECTRICAL DYSSYNCHRONY

CROSS-REFERENCE TO RELATED APPLICATIONS

This application claims the benefit of U.S. Provisional Application No. 61/482,053 filed on May 3, 2011, the entire content of which is incorporated herein by reference.

TECHNICAL FIELD

The disclosure relates to electrophysiology and, more particularly, to evaluating the electrical activation patterns of the heart.

BACKGROUND

The beat of the heart is controlled by the sinoatrial node, a group of conductive cells located in the right atrium near the entrance of the superior vena cava. The depolarization signal generated by the sinoatrial node activates the atrioventricular node. The atrioventricular node briefly delays the propagation of the depolarization signal, allowing the atria to drain, before passing the depolarization signal to the ventricles of the heart. The coordinated contraction of both ventricles drives the flow of blood through the torso of a patient. In certain circumstances, the conduction of the depolarization signal from the atrioventricular node to the left and right ventricles may be interrupted or slowed. This may result in a dyssynchrony in the contraction of the left and right ventricles, and eventually in heart failure or death.

Cardiac Resynchronization Therapy (CRT) may correct the symptoms of electrical dyssynchrony by providing pacing therapy to one or both ventricles or atria, e.g., by providing pacing to encourage earlier activation of the left or right ventricles. By pacing the contraction of the ventricles, the ventricles may be controlled so that the ventricles contract in synchrony. Some patients undergoing CRT have experienced improved ejection fraction, increased exercise capacity, and an improved feeling of well-being.

Providing CRT to a patient may involve determining whether the patient will derive benefit from the CRT prior to implantation of a cardiac rhythm device, determining optimal site for placement of one or more ventricular pacing leads, and programming of device parameters, such as selection of electrodes on multi-polar right or left ventricular leads, as well as selection of the timing of the pacing pulses delivered to the electrodes, such as atrioventricular (A-V) and intra-ventricular (V-V) delays. Assessment of electrical dyssynchrony for these purposes has typically involved assessing QRS duration clinically. Though CRT is recommended typically for patients with wide QRS duration, hemodynamic improvements through CRT have been reported in narrow QRS heart failure patients. Thus, some patients who may benefit from CRT may not be prescribed CRT based on present electrical dyssynchrony evaluation techniques.

SUMMARY

In general, the disclosure is directed towards techniques for evaluating electrical dyssynchrony of the heart of a patient. The evaluation of electrical dyssynchrony may facilitate patient selection for CRT. The evaluation of electrical dyssynchrony may also facilitate placement of implantable leads, e.g., one or more left ventricular leads, and programming of device parameters for CRT during an implantation procedure, or reprogramming of device parameters for CRT during a follow-up visit.

A set of electrodes may be spatially distributed about the torso of a patient. The electrodes may each sense a body-surface potential signal, and more particularly a torso-surface potential signal, which indicates the depolarization signals of the heart of the patient after the signals have progressed through the torso of the patient. Due to the spatial distribution of the electrodes, the torso-surface potential signal recorded by each electrode may indicate the depolarization of a different spatial region of the heart.

In some examples, an activation time is determined for each torso-surface potential signal, i.e., for each electrode of the set. The dispersion or sequence of these activation times may be analyzed or presented to provide variety of indications of the electrical dyssynchrony of the heart of the patient. For example, isochrone or other activation maps of the torso-surface illustrating the activation times may be presented to user to illustrate electrical dyssynchrony of the heart. In some examples, values of one or more statistical indices indicative of the temporal and/or spatial distribution of the activation times may be determined. Such maps and indices, or other indications of dyssynchrony determined based on the torso-surface activation times, may indicate electrical dyssynchrony of the heart to a user, and facilitate evaluation of a patient for CRT, and configuration of CRT for the patient.

In some examples, the locations of all or a subset of the electrodes, and thus the locations at which the torso-surface potential signals were sensed, may be projected on the surface of a model torso that includes a model heart. The inverse problem of electrocardiography may be solved to determine electrical activation times for regions of the model heart based on the torso-surface potential signals sensed from the patient. In this manner, the electrical activity of the heart of the patient may be estimated. Various isochrone or other activation time maps of the surface of the model heart may be generated based on the torso-surface potential signals sensed on the surface of the torso of the patient. Further, values of one or more indices indicative of the temporal and/or spatial distribution of the activation times on model heart may be determined. These measures and representations of electrical dyssynchrony may be used to evaluate the suitability of the patient for CRT, adjust the positioning of the CRT leads during implantation, and determine which electrodes of one or more multi-polar leads should be utilized for delivery of CRT, as well as the timing of pacing pulses, such as atrio-ventricular (A-V) and intra-ventricular (V-V) delays for delivery of CRT to the patient.

For example, the one or more indications of dyssynchrony may be determined or generated based on data collected both during intrinsic conduction and during CRT. The degree of dyssynchrony during intrinsic conduction and CRT may be compared, e.g., to determine whether a patient is a candidate for CRT. Similarly, the one or more indications of dyssynchrony may be determined or generated based on data collected during CRT with different lead positions, different electrode configurations, and/or different CRT parameters, e.g., A-V or V-V delay. The change in dyssynchrony attributable to these different lead positions, different electrode configurations, and/or different CRT parameters may be evaluated.

In one example, a method comprises receiving, with a processing unit, a torso-surface potential signal from each of a plurality of electrodes distributed on a torso of a patient.

The method further comprises for at least a subset of the plurality of electrodes, calculating, with the processing unit, a torso-surface activation time based on the signal sensed from the electrode, and presenting, by the processing unit, to a user, an indication of a degree of dyssynchrony of the torso-surface activation times via a display.

In another example, a system comprises a plurality of electrodes distributed on a torso of a patient, and a processing unit. The processing unit is configured to receive a torso-surface potential signal from each of the plurality of electrodes, calculate, for at least a subset of the plurality of electrodes, a torso-surface activation time based on the signal sensed from the electrode, and present, to a user, an indication of a degree of dyssynchrony of the torso-surface activation times via a display.

In another example a computer-readable storage medium comprises instructions that, when executed, cause a processor to receive a torso-surface potential signal from each of a plurality of electrodes distributed on a torso of a patient, calculate, for at least a subset of the plurality of electrodes, a torso-surface activation time based on the signal sensed from the electrodes, and present to a user, an indication of a degree of dyssynchrony of the torso-surface activation times via a display.

The details of one or more aspects of the disclosure are set forth in the accompanying drawings and the description below. Other features, objects, and advantages will be apparent from the description and drawings, and from the claims.

BRIEF DESCRIPTION OF DRAWINGS

FIG. **1** is a conceptual diagram illustrating an example system that may be used to provide CRT to a heart of a patient.

FIG. **2** is a timing diagram showing an example ECG tracing of two healthy heart beats.

FIG. **3** is a timing diagram showing an example ECG tracing of a patient suffering from left bundle branch block.

FIGS. **4**A and **4**B are conceptual diagrams illustrating example systems for measuring torso-surface potentials.

FIG. **5** is a block diagram illustrating an example system for measuring torso-surface potentials.

FIG. **6** is a series of simulated isochrone maps of torso-surface activation times for typical left bundle branch block intrinsic rhythm and CRT pacing.

FIG. **7** is a flow diagram illustrating an example operation of a system to provide indications of the cardiac electrical dyssynchrony of a patient based on torso-surface activation times.

FIG. **8** is a flow diagram illustrating an example technique for prescribing and configuring CRT based on an assessment cardiac electrical dyssynchrony of a patient via the torso-surface activation times.

FIG. **9** is a series of isochrone maps of cardiac activation times constructed with two different heart-torso models using body-surface ECG data from the same patient.

FIG. **10** is a flow diagram illustrating an example operation of a system to measure the cardiac electrical dyssynchrony of a patient via the cardiac activation times.

FIG. **11** is a flow diagram illustrating an example technique for configuring CRT based on an assessment of cardiac electrical dyssynchrony of a patient via the cardiac activation times.

DETAILED DESCRIPTION

FIG. **1** is a conceptual diagram illustrating an example system that may be used to provide CRT to heart **10** of patient 1. The system may include an implantable medical device (IMD) **100**. IMD **100** may be a CRT pacemaker or CRT defibrillator. IMD **100** may be equipped with one or more leads; leads **102**, **104**, and **106**; that are inserted into or on the surface of the left ventricle **12**, right ventricle **14**, or right atrium **16** of heart **10**. Leads **102**, **104**, and **106** may be equipped with one or more electrodes **108**, **110**, and **112**.

Heart **10** may suffer from an electrical dyssynchrony. Electrical dyssynchrony may occur when the depolarization signals that start the contraction of ventricles **12** and **14** do not reach the ventricles in a coordinated manner, and results in an inefficient pumping action of heart **10**. Patient 1 may experience symptoms of heart failure. Electrical dyssynchrony may be caused by damage to the electrical system of heart **10**, e.g., a bundle branch block or damage to the fascicle of heart **10**. Alternate conduction pathways may form within heart **10**, but these pathways may slow the progress of the electrical depolarization signal and result in the asynchronous contraction of ventricles **12** and **14**.

IMD **100** may provide CRT stimulation to heart **10** of patient 1. IMD **100** is depicted as being configured to deliver stimulation to right atrium **16**, right ventricle **14**, and left ventricle **12** of heart **10**. In other examples, IMD **100** may be configured to deliver stimulation to other portions of heart **10** depending on the condition of patient 1. IMD **100** may interact with an external programmer (not shown) to adjust operating characteristics, such as A-V and V-V delays, of the therapy delivered by IMD **100**. In some examples, IMD **100** may also be configured to sense the electrical activity of heart **10** through the electrodes on one or more of leads **102**, **104**, and **106**.

As shown in FIG. **1**, leads **102**, **104**, **106** may extend into the heart **10** of patient 1 to deliver electrical stimulation to heart **10** and synchronize the contraction of ventricles **12** and **14**. Right ventricular lead **106** extends through one or more veins (not shown), the superior vena cava (not shown), and right atrium **16**, and into right ventricle **14**. Left ventricular coronary sinus lead **102** extends through one or more veins, the vena cava, right atrium **16**, and into the coronary sinus (not shown) to a region adjacent to the free wall of left ventricle **12** of heart **10**. Right atrial lead **104** extends through one or more veins and the vena cava, and into the right atrium **16** of heart **10**.

In other configurations, IMD **100** may be equipped with more or fewer leads, depending on the requirements of the therapy provided to patient 1. For example, IMD **100** may be equipped with leads that extend to greater or fewer chambers of heart **10**. In some example, IMD **100** may be equipped with multiple leads that extend to a common chamber of heart, e.g., multiple leads extending to the left ventricle **12**. IMD **100** may also be equipped with one or more leads that are placed on the heart through other means providing access to the cardiac tissue, such as surgical epicardial lead placement, and other pericardial access approaches. In some examples, IMD **100** may be equipped with a left ventricular lead that is placed on the heart endocardially. Additionally, although illustrated as implanted on the right side of patient 1 in FIG. **1**, IMD **100** may in other examples be implanted on the left side of the pectoral region of the patient, or within the abdomen of the patient.

Electrodes **108**, **110**, and **112** may attach to portions of heart **10** to provide electrical stimulation or sense the electrical depolarization and repolarization signals of heart **10**. Electrode **108**, in right ventricle **14**, may be affixed to the wall of heart **10** via a screw based mechanism. Electrode **110** may comprise multiple electrodes mounted the same lead, allowing lead **102** to both transmit therapeutic shocks as

well as electrical sense data detected by electrode **110**. Electrodes **110** and **112** may be attached to the surface of heart **10** via glue, barbs, or another permanent or semi-permanent attachment mechanism.

FIG. **2** is a timing diagram showing an example ECG tracing **200** in conjunction with certain periods or phases of the mechanical cardiac cycle. The depiction and associated description of FIG. **2** are generalized in the sense that the relationship between the timing of electrical and mechanical events is not necessarily as described for all subjects, or at all times for any given subject.

ECG tracing **200** depicts the electrical signal of two example healthy cardiac cycles. The electrical signal of a healthy heart comprises a series of 5 characteristic waves: the P-wave, Q-wave, R-wave, S-wave, and T-wave. Each of these waves, and the intervals between them, correspond to discrete events in the functioning of a healthy heart.

In general, at some point during period **202**, which stretches from the peak of a P-wave to the peak of the subsequent R-wave, atrial systole occurs, which is the contraction of the atria that drives blood from the atria into the ventricles. Period **204**, from the peak of the R-wave to the opening of the aortic valve, generally marks a period of isovolumetric contraction. The atrioventricular and aortic valves are closed, preventing blood flow and leading to an increase in pressure in the ventricles but not yet in the aorta. Period **206**, bounded by the opening and closing of the aortic valves is generally when ejection occurs during the cardiac cycle. During ejection period **206** the ventricles contract and empty of blood, driving the blood into cardiovascular system. As the contraction of the ventricles complete, the pressure of the blood within the cardiovascular system closes the aortic valves. Period **208**, bounded by the closing of the aortic valves and the opening of the atrioventricular valves, is the isovolumetric relaxation of the ventricles. Periods **210** and **212** are collectively known as the late diastole, where the whole heart relaxes and the atria fill with blood. Period **210** corresponds to a rapid inflow of blood while period **212** corresponds to diastasis, the period of slower flow blood into the atria before the atrial systole **202** occurs again.

The P-wave marks the stimulation of the atria and the beginning of the cardiac cycle. The atria contract under the stimulation, forcing blood into the ventricles. The PR segment marks the delay as the depolarization signal travels from the atrioventricular node to the Purkinje fibers. The Q-wave marks the depolarization of the interventricular septum as an initial part of the depolarization of the ventricles. The R-wave follows the Q-wave and represents the depolarization of the ventricles. The S-wave follows the R-wave and represents the later depolarization of the ventricles. The T-wave marks the recovery and repolarization of the ventricles in preparation for the next beat of the heart.

The QRS complex, spanning from the beginning of the Q-wave to the end of the S-wave, represents the electrical activation of the myocardium. Ventricular contraction of both the left and right ventricles is in response to the electrical activation. The QRS complex typically lasts from 80 to 120 ms. The relatively large amplitude of the QRS complex is due to the large muscle mass of the ventricles. Issues affecting the synchrony of the ventricular contraction may be demonstrated in the deformation of the QRS complex. For example, electrical dyssynchrony in the contraction of the ventricles can widen the R-wave or produce two R-wave peaks, typically labeled the r-wave and R'-wave, corresponding to the depolarization of each ventricle. The S-wave and the T-wave may be morphological different than in an ECG tracing of a healthy heart.

FIG. **3** is a timing diagram showing ECG tracing **300**. ECG tracing **300** depicts the electrical signal of a patient suffering from a left bundle branch block. A sign of the condition is the presence of an rS complex versus the typical QRS complex, though other variations of Q, R, and S waves form combinations that may be present in patients suffering from a left bundle branch block, right bundle branch blocks, or other ventricular conduction conditions. The extended duration of the rS complex indicates an extended ventricular contraction time, likely due to electrical dyssynchronies.

Diagnosis of a left or right bundle branch block, or cardiac electrical dyssyncrony in general, typically involves measuring the duration of the QRS complex (or other complex marking the depolarization of the ventricles). QRS complexes lasting 100 ms or longer may indicate a partial bundle branch block and 120 ms or longer a complete bundle branch block. In FIG. **3**, the initial Q-wave is not visible, instead the tracing shows an initial r-wave, corresponding to the initial depolarization of the right ventricle and followed by an S-wave marking the rapid depolarization of both ventricles after the cardiac signal has reached the left ventricle after traveling through the myocardium of the heart, rather than through the bundle branches. Because the myocardium conducts electricity more slowly than the bundle branches, the entire complex is spread out over a longer period.

Absent a case of bundle branch block—such as the one shown in FIG. **3**—or other condition, diagnosis may be more challenging. Occult dyssynchronies may be present that, while responsive to CRT, may not be readily identifiable from an examination of the typical 12-lead ECG. These occult dyssynchronies may manifest in the electrical signals generated by the heart and measured on the surface of the torso and may be diagnosable through alternative means of analysis, such as by determining cardiac activation times at a plurality of spatially distributed locations according to the techniques described herein.

FIGS. **4**A and **4**B are conceptual diagrams illustrating example systems for measuring body-surface potentials and, more particularly, torso-surface potentials. In one example illustrated in FIG. **4**A, sensing device **400**A, comprising a set of electrodes **404**A-F (generically "electrodes **404**") and strap **408**, is wrapped around the torso of patient 1 such that the electrodes surround heart **10**. As illustrated in FIG. **4**A, electrodes **404** may be positioned around the circumference of patient 1, including the posterior, lateral, and anterior surfaces of the torso of patient 1. In other examples, electrodes **404** may be positioned on any one or more of the posterior, lateral, and anterior surfaces of the torso. Electrodes **404** may be electrically connected to processing unit **500** via wired connection **406**. Some configurations may use a wireless connection to transmit the signals sensed by electrodes **404** to processing unit **500**, e.g., as channels of data.

Although in the example of FIG. **4**A sensing device **400**A comprises strap **408**, in other examples any of a variety of mechanisms, e.g., tape or adhesives, may be employed to aid in the spacing and placement of electrodes **404**. In some examples, strap **408** may comprise an elastic band, strip of tape, or cloth. In some examples, electrodes **404** may be placed individually on the torso of patient 1.

Electrodes **404** may surround heart **10** of patient 1 and record the electrical signals associated with the depolarization and repolarization of heart **10** after the signals have propagated through the torso of patient 1. Each of electrodes **404** may be used in a unipolar configuration to sense the

torso-surface potentials that reflect the cardiac signals. Processing unit **500** may also be coupled to a return or indifferent electrode (not shown) which may be used in combination with each of electrodes **404** for unipolar sensing. In some examples, there may be 12 to 16 electrodes **404** spatially distributed around the torso of patient 1. Other configurations may have more or fewer electrodes **404**.

Processing unit **500** may record and analyze the torso-surface potential signals sensed by electrodes **404**. As described herein, processing unit **500** may be configured to provide an output to a user indicating the electrical dyssynchrony in heart **10** of patient 1. The user may make a diagnosis, prescribe CRT, position therapy devices, e.g., leads, or adjust or select treatment parameters based on the indicated electrical dyssynchrony.

In some examples, the analysis of the torso-surface potential signals by processing unit **500** may take into consideration the location of electrodes **404** on the surface of the torso of patient 1. In such examples, processing unit **500** may be communicatively coupled to an imaging device **501**, which may provide an image that allows processing unit **500** to determine coordinate locations of each of electrodes **400** on the surface of patient 1. Electrodes **404** may be visible, or made transparent through the inclusion or removal of certain materials or elements, in the image provided by imaging system **501**.

FIG. **4**B illustrates an example configuration of a system that may be used to evaluate electrical dyssynchrony in heart **10** of patient 1. The system comprises a sensing device **400**B, which may comprise vest **410** and electrodes **404** A-ZZ (generically "electrodes **404**"), a processing unit **500**, and imaging system **501**. Processing unit **500** and imaging system **501** may perform substantially as described above with respect to FIG. **4**A. As illustrated in FIG. **4**B, electrodes **404** are distributed over the torso of patient 1, including the anterior, lateral, and posterior surfaces of the torso of patient 1.

Sensing device **400**B may comprise a fabric vest **410** with electrodes **404** attached to the fabric. Sensing device **400**B may maintain the position and spacing of electrodes **404** on the torso of patient 1. Sensing device **400**B may be marked to assist in determining the location of electrodes **404** on the surface of the torso of patient 1. In some examples, there may be 150 to 256 electrodes **404** distributed around the torso of patient 1 using sensing device **400**B, though other configurations may have more or fewer electrodes **404**.

FIG. **5** is a block diagram illustrating an example system for measuring torso-surface potentials and providing indications of electrical dyssynchrony. The example system may comprise a processing unit **500** and a set of electrodes **404** on a sensing device **400**, e.g., one of example sensing devices **400**A or **400**B (FIGS. **4**A and **4**B). The system may also include an imaging system **501**.

As illustrated in FIG. **5**, processing unit **500** may comprise a processor **502**, signal processor **504**, memory **506**, display **508**, and user input device **509**. Processing unit **500** may also include an electrode location registration module **524**. In the illustrated example, processor **502** comprises a number of modules and, more particularly, a projection module **514**, an inverse problem module **516**, an activation time module **518**, an indices module **520**, and an isochrones mapping module **522**. Memory **506** may store recorded data **510** and models **512**.

Processing unit **500** may comprise one or more computing devices, which may be co-located, or dispersed at various locations. The various modules of processing unit **500**, e.g., processor **502**, projection module **514**, inverse problem module **516**, activation time module **518**, statistics module **520**, isochrones mapping module **522**, signal processor **504**, electrode location registration module **524**, display **508**, memory **506**, recorded data **510** and torso models **512** may be implemented in one or more computing devices, which may be co-located, or dispersed at various locations. Processor **502**, and the modules of processor **502**, may be implemented in one or more processors, e.g., microprocessors, of one or more computing devices, as software modules executed by the processor(s). Electrode location registration module **524** may, in some examples, be implemented in imaging system **501**.

In addition to the various data described herein, memory **506** may comprise program instructions that, when executed by a programmable processor, e.g., processor **502**, cause the processor and any components thereof to provide the functionality attributed to a processor and processing unit herein. Memory **506** may include any volatile, non-volatile, magnetic, optical, or electrical media, such as a hard disk, magnetic tape, random access memory (RAM), read-only memory (ROM), CD-ROM, non-volatile RAM (NVRAM), electrically-erasable programmable ROM (EEPROM), flash memory, or any other digital or analog media. Memory **506** may comprise one or more co-located or distributed memories. Memory **506** may comprise a tangible article that acts as a non-transitory storage medium for data and program instructions.

The torso-surface potential signals sensed by electrodes **404** of sensing device **400** may be received by signal processor **504** of processing unit **500**. Signal processor **504** may include an analog-to-digital converter to digitize the torso-surface potential signals. Signal processor **504** may also include various other components to filter or otherwise condition the digital signals for receipt by processor **502**.

Electrode location registration module **524** may receive imaging data from imaging system **501**. Electrode location registration module **524** analyzes the imaging data. In particular, electrode registration location module **524** identifies electrodes **404**, or elements co-located with the electrodes that are more clearly visible via the imaging modality, within the images. Electrode location registration module **524** may further identify the locations of each of the electrodes on the surface of the patient and/or within a three-dimensional coordinate system. In some examples, the locations of electrodes **404** may be manually identified and registered with processing unit **500**, e.g., by a user, via electrode registration module **524**.

The imaging data may comprise data representing one or more images of patient 1 wearing electrodes **404**, e.g., of a sensing device **400**. In some examples, the images may be obtained before or during a medical procedure, e.g., a surgical procedure to implant a cardiac rhythm device and lead system for delivery of CRT.

In some examples, processor **502** may store the torso-surface potential signals, imaging data from imaging system, electrode location data from electrode location registration module, or any values disclosed herein that are derived by processing of such signals and data by processor **502**, within memory **506** as recorded data **510**. Each recorded torso-surface potential signal, or other values derived therefrom, may be associated with a location of the electrode **404** that sensed the torso-surface potential signal. In this manner, the torso-surface potential data may be correlated with the position of electrodes **404** on the torso of patient 1, or within a three-dimensional coordinate system, enabling spatial mapping of the data to particular locations on the surface of the torso or within the coordinate system. In some examples,

aspects of the techniques described herein may be performed at some time after the acquisition of the torso-surface potential signals and location data based on recorded data **510**.

Processor **502** may be configured to provide one or more indications of electrical dyssynchrony based on the torso-surface potential signals and, in some examples, the electrode location data. Example indications of electrical dyssynchrony include indices illustrating activation times for each electrode/location distributed about the torso or heart, or for one or more subsets of electrodes located within a common region, e.g., within a left posterior, left anterior, right posterior, or right anterior region. In some examples, processor **502** may be configured to provide a set of two or more different indications, e.g., several different indications, for each of two or more different regions, e.g., several different regions, of the torso or heart.

Some indications of dyssynchrony may include statistical values or other indices derived from activation times for each electrode location or one or more subsets of electrodes within one or more regions. Other examples indications of electrical dyssynchrony that may be determined based on activation times at various electrodes/locations include graphical indications, such as an isochrone or other activation maps, or an animation of electrical activation. Other examples indications of electrical dyssynchrony that may be determined based on activation times at various electrodes/locations include identifying one of a predetermined number of dyssynchrony levels, e.g., high, medium, or low, via text or color, e.g., red, yellow, green, for example.

In some examples, the various indications of dyssynchrony for one or more regions may be determined based on data collected at two or more different times and/or under two or more different conditions. For example, the various indications of dyssynchrony may be determined based on torso-potential signals collected during intrinsic conduction of heart **10**, and also determined based on torso-potential signals collected during CRT. In this manner, the potential dyssynchrony-reducing benefit of CRT may be evaluated for the patient by comparing the different values, graphical representations, or the like, resulting from intrinsic conduction and CRT. As another example, the various indications of dyssynchrony may be determined each of a plurality of different times based on torso-potential signals collected during delivery of CRT with different lead positions, electrode configurations, or CRT parameters, e.g., A-V or V-V interval values. In this manner, the relative dyssynchrony-reducing benefits of the different lead positions, electrode configurations, or CRT parameters positions may be evaluated for the patient by comparing the different values, graphical representations, or the like.

Models **512** may include a plurality of different models, e.g., three-dimensional models, of the human torso and heart. A model torso or model heart may be constructed by manual or semi-automatic image segmentation from available databases of previously acquired medical images (CT/MRI) of a plurality of subjects, e.g., cardiomyopathy patients, different than patient 1, using commercially available software. Each model may be discretized using a boundary element method. A plurality of different torso models may be generated. The different models may represent different subject characteristics, such as different genders, disease states, physical characteristics (e.g., large frame, medium frame and small frame), and heart sizes (e.g., x-large, large, medium, small). By providing input via user input **509**, a user may select from among the various model torsos and model hearts that may be stored as models **512** in memory **506**, so that the user may more closely match the actual torso and heart **10** of patient 1 with the dimensions and geometry of a model torso and model heart. In some examples, medical images of the patient, e.g., CT or MRI images, may be manually or semi-automatically segmented, registered, and compared to models **512** for selection from amongst the models **512**. Furthermore, single or multiple view 2-D medical images (e.g., x-ray, fluoroscopy) may be segmented or measured to determine approximate heart and torso dimensions specific to the patient in order to select the best fit model torso and heart.

Projection module **514** may project the locations of electrodes **404**, e.g., stored as recorded data **510** within of memory **506**, onto an appropriate, e.g., user-selected, model torso contained in model data module **512** of memory **506**. By projecting the location of electrodes **404** onto the model torso, projection module **514** may also project the torso-surface potential signals of patient 1 sensed by electrodes **404** onto the model torso. In other examples, the measured electrical potentials may be interpolated and resamples at electrode positions given by the model. In some examples, projecting the torso-surface potentials onto the model torso may allow processor **502**, via inverse problem module **516**, to estimate the electrical activity of at various locations or regions of the model heart corresponding to heart **10** of patient 1 that produced the measured torso-surface potentials.

Inverse problem module **516** may be configured to solve the inverse problem of electrocardiography based on the projection of the measured torso-surface potentials, recorded by electrodes **404**, onto the model torso. Solving the inverse problem of electrocardiography may involve the estimation of potentials or activation times in heart **10** based on a relationship between the torso and heart potentials. In one example method, model epicardial potentials are computed from model torso potentials assuming a source-less volume conductor between the model heart and the model torso in an inverse Cauchy problem for Laplace's equation. In another example method, an analytic relationship between torso-surface potentials and the cardiac transmembrane potential is assumed. Torso-surface potentials may be simulated based on this relationship. In some examples, inverse problem module **516** may utilize techniques described by Ghosh et al. in "Accuracy of Quadratic Versus Linear Interpolation in Non-Invasive Electrocardiographic Imaging (ECGI)," Annals of Biomedical Engineering, Vol. 33, No. 9, September 2005, or in "Application of the L1-Norm Regularization to Epicardial Potential Solution of the Inverse Electrocardiography Problem," Annals of Biomedical Engineering, Vol. 37, No. 5, 2009, both of which are incorporated herein by reference in their entireties. In other examples, any known techniques for solving the inverse problem of electrocardiography may be employed by inverse problem module **516**.

Activation time module **518** may compute the activation times directly from measured torso-surface potentials, or by estimating model transmembrane potentials. In either case, an activation time for each electrode/location may be determined as a time period between two events, such as between the QRS complex onset and the minimum derivative (or steepest negative slope) of the sensed torso potential signal or estimate epicardial potential signal. Thus, in one example, cardiac activation times are estimated from the steepest negative slope of the model epicardial electrograms. Cardiac activation times (parameters in the analytic relationship between torso-surface potential and cardiac transmembrane potential) may, in other configurations, be computed based on minimizing the least square difference between the

measured torso-surface potentials and simulated torso-surface potentials. A color-coded isochrone map of ventricular, epicardial, or torso-surface activation times may be shown by display **308**. In other examples, display **308** may show a two-color animation of propagation of the activation wavefront across the surface of the model heart or the torso-surface.

Indices module **520** may be configured to compute one or more indices of electrical dyssynchrony from the torso-surface or cardiac activation times. These indices may aid in the determination of whether the patient is a candidate for CRT, placement of CRT leads, and selection of CRT parameters. For example, LV lead **102** (FIG. **1**) may be positioned at the site that reduces dyssynchrony from one or more indices or, alternatively, the largest electrical resynchronization as demonstrated by the indices. The same indices may be also used for programming A-V and/or V-V delays during follow-up. As indicated above, the indices may be determined based on the activation times for all electrodes/locations, or for one or more subsets of electrodes in one or more regions, e.g., to facilitate comparison or isolation of a region, such as the posterior and/or left anterior, or left ventricular region.

One of the indices of electrical dyssynchrony may be a standard deviation index computed as the standard deviation of the activations-times (SDAT) of some or all of electrodes **404** on the surface of the torso of patient 1. In some examples, the SDAT may be calculated using the estimated cardiac activation times over the surface of a model heart.

A second example index of electrical dyssynchrony is a range of activation times (RAT) which may be computed as the difference between the maximum and the minimum torso-surface or cardiac activation times, e.g., overall, or for a region. The RAT reflects the span of activation times while the SDAT gives an estimate of the dispersion of the activation times from a mean. The SDAT also provides an estimate of the heterogeneity of the activation times, because if activation times are spatially heterogeneous, the individual activation times will be further away from the mean activation time, indicating that one or more regions of heart **10** have been delayed in activation. In some examples, the RAT may be calculated using the estimated cardiac activation times over the surface of a model heart.

A third example index of electrical dyssynchrony estimates the percentage of electrodes **404** located within a particular region of interest for the torso or heart, whose associated activation times are greater than a certain percentile, for example the 70th percentile, of measured QRS complex duration or the determined activation times for electrodes **404**. The region of interest may be a posterior, left anterior, and/or left-ventricular region, as examples. This index, the percentage of late activation (PLAT), provides an estimate of percentage of the region of interest, e.g., posterior and left-anterior area associated with the left ventricular area of heart **10**, which activates late. A large value for PLAT may imply delayed activation of substantial portion of the region, e.g., the left ventricle **12** (FIG. **1**), and the potential benefit of electrical resynchronization through CRT by pre-exciting the late region, e.g., of left ventricle **12**. In other examples, the PLAT may be determined for other subsets of electrodes in other regions, such as a right anterior region to evaluate delayed activation in the right ventricle. Furthermore, in some examples, the PLAT may be calculated using the estimated cardiac activation times over the surface of a model heart for either the whole heart or for a particular region, e.g., left or right ventricle, of the heart.

Isochrone module **522** may be configured to generate an isochrone map depicting the dispersion of activation times over the surface of the torso of patient 1 or a model heart. Isochrone module **522** may incorporate changes in the torso-surface or cardiac activation times in near real-time, which may permit near instant feedback as a user adjusts a CRT device or monitors patient 1 to determine if CRT is appropriate. Isochrone maps generated by isochrone module **522** may be presented to the user via display **508**.

In general, processor **502** may generate a variety of images or signals for display to a user via display **508** based on the measured torso-surface potentials, calculated torso-surface or estimated cardiac activation times, or the degree of change in electrical dyssynchrony. For example, a graded response reflecting the efficacy of a particular location of the LV lead **102** during biventricular pacing or single ventricle fusion pacing may be provided to the physician in terms of a red, yellow and green signal. A red signal may be shown if the reduction in electrical dyssynchrony during CRT pacing compared to intrinsic rhythm is negative (an increase in electrical dyssynchrony) or minimal, e.g., less than 5%. A yellow signal may be triggered if there is some reduction in electrical dyssynchrony during CRT pacing compared to intrinsic rhythm, for example between 5% and 15%, but there may be potentially better sites for lead placement. If the reduction in electrical dyssynchrony during CRT pacing compared to intrinsic rhythm is substantial, e.g., greater than 15%, a green signal may be triggered indicating to the physician that the present site provides effective changes in synchronization. The feedback from this system in combination with other criteria (like magnitude of pacing threshold, impedance, battery life, phrenic nerve stimulation) may be also used to choose an optimal pacing vector for one or more multipolar leads. The feedback from this system may be also used for selecting optimal device timings (A-V delay, V-V delay, etc) influencing the extent of fusion of intrinsic activation with paced activation from single or multiple ventricular sites, or discerning acute benefit of single site fusion pacing versus multi-site pacing and choice of appropriate pacing type.

Display **508** may also display three-dimensional maps of electrical activity over the surface of the torso of patient 1 or over a model heart. These maps may be isochrone maps showing regions of synchronous electrical activity as the depolarization progresses through heart **10** of patient 1. Such information may be useful to a practitioner in diagnosing asynchronous electrical activity and developing an appropriate treatment, as well as evaluating the effectiveness of the treatment.

FIG. **6** is a series of simulated isochrone maps **600** of torso-surface activation times over the torso of a patient suffering from an electrical dyssynchrony in the left ventricle before and during treatment with a CRT device. The isochrone maps before (intrinsic) and after treatment are divided into two views: anterior and posterior. Line **602** represents the location of a subset of electrodes **404**, e.g., a subset of electrodes **404** of sensing device **400**B, that may be used to calculate one or more indices of electrical dyssynchrony. In some examples, line **602** may represent electrodes **404** on sensing device **400**A.

The isochrone maps **600** of the natural and CRT assisted torso-surface activation times may be generated using multiple electrodes **404** distributed over the surface of the torso of a patient, e.g., using sensing device **400**B. Generation of the isochrone maps **600** may include determining the location of electrodes **404**, and sensing torso-surface potential signals with the electrodes. Generation of the isochrone

maps **600** may further include calculating the torso-surface activation time for each electrode or electrode location by determining the point in the recorded QRS complex of the signal sensed by the electrodes corresponding to the maximum negative slope. In other examples, the torso-surface activation times may be determined by identifying the minimum derivative of the QRS complex. The measured torso-surface activation times may then be standardized and an isochrone map of the surface of the torso of the patient generated.

The delayed activation of certain locations associated with certain ones of electrodes **404** due to the electrical dyssynchrony is apparent in the posterior views of the intrinsic torso-surface activation times. Regions **604** indicate increased delay in the activation of the underlying heart. The corresponding posterior view during treatment with a CRT device indicate that regions **606**, the same location as regions **604** on the maps of intrinsic torso-surface activation times, exhibits increased synchrony in electrical ventricular activity. The CRT maps exhibit decreased range and a lower standard deviation of torso-surface activation times. Further, the posterior regions no longer exhibit delayed activation times. The isochrone map of the torso-surface activation times during intrinsic and CRT pacing and changes in distribution of activation-times from intrinsic to CRT pacing may be used for diagnostic purposes or the adjustment of a CRT device.

One or more indices of electrical dyssynchrony may also be calculated from the torso-surface activation times used to generate isochrone maps **600**. For example, SDAT, an indication of the spread of the activation times, for the patient's intrinsic heart rhythm using the complete set of electrodes **404** is 64. Using the reduced lead set marked by line **602** results in an SDAT of 62. The RAT for the intrinsic heart rhythm and complete lead set is 166.5 while the reduced lead set has a RAT of 160. PLAT for the intrinsic heart rhythm using the reduced and complete lead sets are 56.15% and 66.67%, respectively. This indicates that using a reduced lead set that circumscribes the heart of the patient, e.g., sensing device **400**A and associated electrodes **404**, may provide comparable indices of electrical dyssynchrony compared to using an electrode set covering the torso of the patient, such as sensing device **400**B.

The indices of electrical dyssynchrony also provide indication of the effectiveness of the CRT device, with the SDAT for the reduced set of electrodes declining to 24, the RAT to 70 and PLAT to 36%. This indicates that the torso-surface activation times during CRT treatment were more narrowly distributed and in a smaller range than in the normal heart rhythm and that the percentage of electrodes **404** located on the left anterior surface of the torso of the patient registering late activation times decreased markedly.

FIG. **7** is a flow diagram illustrating an example operation of a system to evaluate the cardiac electrical dyssynchrony of a patient via the torso-surface activation times. The location of electrodes, e.g., electrodes **404** (FIGS. **4**A and **4**B), distributed over the surface of the torso of the patient may be determined (**700**). A cardiac event, e.g., a depolarization, may generate an electrical signal that propagates through the torso of a patient, e.g., patient 1 (FIG. **1**) and registers on the electrodes. The signal sensed by the electrodes may be received (**702**), e.g., by processing unit **500** (FIG. **5**). The processing unit may calculate the torso-surface activation times (**704**). In some examples, the processing unit may also construct a torso-surface activation times isochrone map (**706**). The processing unit may also calculate at least one index of cardiac electrical dyssynchrony (**708**). These indices may comprise one or more of the SDAT (**710**), RAT (**712**), and the PLAT (**714**).

A cardiac event, such as a depolarization, generates an electrical signal that propagates through the torso. The electrical signal may comprise a QRS complex, or a variant caused by a heart related condition such as a left or right bundle branch block. The electrical signal may not propagate uniformly through the torso of a patient due to variations in conductivity within the torso and the heart. These delays may manifest in electrodes distributed over the surface of the torso of the patient registering the same electrical signal at different points in time.

The electrical signal generated by the cardiac event may register on the plurality of electrodes distributed over the surface of the torso of patient. The electrodes may be distributed over the anterior, lateral, and/or posterior surfaces of the torso, allowing the generation of a three-dimensional picture of the electrical activity occurring within the torso. In some examples, the electrodes may be placed to provide extensive coverage both above and below the heart, e.g., by using sensing device **400**B (FIG. **4**B). In other examples, a reduced set of electrodes may be arranged around the circumference of the torso, circumscribing the heart of the patient, e.g., using sensing device **400**A (FIG. **4**A). The electrodes may receive the complete waveform of the electrical signal generated by the cardiac event, and transmit the signal to a processing unit.

The location of electrodes distributed over the surface of the torso of the patient may be determined (**700**). Locating the electrodes may be performed automatically, e.g. by imaging system **501** and electrode location registration module **524** of processing unit **500** (FIG. **5**). The electrodes may be located by analyzing one or more images of the torso of a patient and performing a pattern matching routine, e.g., recognizing the shape of an electrode against the torso of the patient, and storing the location of the electrode on the torso of the patient in processing unit memory. In other examples, the location of sensing device **400**A or **400**B may be determined and the locations of the electrodes determined based on the position of the sensing device, e.g., basing the position of the electrode on the patient through the known position of the electrode on the sensing device. In another example, the position of the electrodes may be measured manually.

The processing unit may receive the electrical signal from the electrodes and record the output in memory (**702**). The processing unit may record the raw output, e.g., the raw ECG tracing from each electrode, as well as location data for the electrodes, allowing the electrical signals detected by the electrodes to be mapped onto the surface of the torso of the patient.

The processing unit may compute the torso-surface activation times (**704**). A processor, e.g., processor **502** of processing unit **500** (FIG. **5**), may retrieve ECG tracing data stored within the processing unit memory and analyze the tracing to detect depolarization of the ventricles of the heart, typically marked by a QRS complex in the tracing. The processor may, in some examples, detect ventricular depolarization by determining the time of the minimum derivative (or steepest negative slope) within the QRS complex measured with respect to the time of QRS complex onset. The determination of the activation time may be made for each electrode and stored in the processing unit memory.

In some configurations, the processing unit may construct an isochrone map of the torso-surface activation times, allowing the user to visually inspect the propagation of the electrical signals of the heart after progression through the

torso of the patient. The isochrone map may be constructed by dividing the range of measured torso-surface activation times into a series of sub-ranges. The location of each electrode on the surface of the torso of the patient may be graphically represented. Regions of electrodes whose measured activation times fall within the same sub-range may be represented by the same color on the graphical representation.

The processing unit may also calculate one or more indices of electrical dyssynchrony based on the torso-surface activation times (**708**). These indices may include the SDAT (**710**), RAT (**712**), and PLAT (**714**). In some examples, the PLAT may be determined as the percentage of posterior electrodes activating after a certain percentage of the QRS complex duration.

As discussed above, in some examples, the construction of a torso-surface activation times isochrone map (**706**), or other graphical representation of dyssynchrony, as well as the calculation of indices of electrical dyssynchrony (**708**), may be performed for a particular region of the torso based the signals received from electrodes (**702**) in such regions. Graphical representations and indices of electrical dyssynchrony may be determined for each of a plurality of regions based on the signals received from the electrodes for such regions. In some examples, the representations and indices for various regions may be presented together or compared.

FIG. **8** is a flow diagram diagram illustrating an example technique for measuring the cardiac electrical dyssynchrony of a patient via measured torso-surface activation times. A processing unit **500** may receive torso-surface potential signals from a plurality of electrodes (**800**), e.g., electrodes **404** (FIGS. **4**A and **4**B). The processing unit **500** may calculate the torso-surface activation times for each of the plurality of electrodes (**802**). The processing unit **500** may provide at least one indication of cardiac electrical dyssynchrony (**804**).

A user may evaluate the whether a patient is a candidate for CRT based on the at least one indication of electrical dyssynchrony (**806**). The user may also monitor the at least one indication of electrical dyssynchrony (**808**), and use the changes in the at least one indication to aid in adjusting the positioning of electrodes, e.g., electrodes **108**, **110**, and **112** (FIG. **1**), during implantation of a CRT device (**810**), e.g., IMD **100** (FIG. **1**), or selection of the various programmable parameters, such as electrode combination and the A-V or V-V pacing intervals, of the CRT device (**812**), during implantation or a follow-up visit.

The various indications of cardiac electrical dyssynchrony described herein, such as statistical or other indices, or graphical representations of activation times, may indicate the presence of damage to electrical conductivity of the heart of the patient, for example the presence of a left or right bundle branch block, that may not be apparent from the examination of a standard 12-lead ECG readout. For example, a large SDAT indicates that the activation of the ventricles is occurring over a large time span, indicating that the depolarization of the ventricles is not occurring simultaneously. A large RAT also indicates a broad range of activation times and asynchronous contraction of the ventricles. A high PLAT indicates that a specific region of the heart, e.g., the posterior regions associated with the left ventricle, may be failing to activate in concert with the measured QRS complex. Additionally, by monitoring the at least one indication of cardiac electrical dyssynchrony, the user may detect changes in the electrical activity of the heart caused by different treatments or treatment configurations.

As described above, the various indications of electrical dyssynchrony, such as statistical indexes, may be calculated for each of a plurality of regions, e.g., posterior, left anterior, or the like, based on torso-surface activations times from the region. Additionally, evaluating whether a patient is a candidate for CRT based on the at least one indication of electrical dyssynchrony (**806**) may include determining the one or more indications of electrical dyssynchrony based on torso-surface activation times both during intrinsic conduction of the heart, and during CRT. Differences between the indications during intrinsic conduction and CRT may indicate that CRT would provide benefit for the patient, e.g., that the patient is a candidate for CRT. As described above, the user may also evaluate whether a patient is a candidate for CRT based on at least one indication of electrical dyssynchrony based on intrinsic rhythm alone. Furthermore, monitoring the at least one indication of electrical dyssynchrony (**808**) during implantation or a follow-up visit may include determining the one or more indications of electrical dyssynchrony for each of a plurality of lead positions, electrode configurations, or other parameter values based on torso-surface activation times resulting from delivery of CRT at the positions, or with the electrode configurations or parameter values. In this manner, differences between dyssynchrony indications associated with various locations, electrode configurations, or parameter values may be compared to determine preferred locations, configurations, or values.

FIG. **9** is a series of isochrone maps of cardiac activation times. Views **900**, **902** and **904** were constructed using torso-surface potentials measured on the surface of the torso of a patient and projected onto three dimensional models of the torso and the heart of the patient. Views **910**, **912**, and **914** were constructed using the measured torso-surface potentials of the same patient projected onto a different model torso and model heart.

The three-dimensional representation of the hearts depicted in views **900**, **902**, **904**, **910**, **912** and **914** were constructed using computer tomography (CT) images of hearts obtained from databases of previously acquired cardiothoracic images. The locations of the electrodes, e.g., electrodes **404** of sensing device **400**B (FIG. **4**B), on the torso of the patient may be plotted to approximate locations on a model torso. A computer may be used to solve the inverse problem of electrocardiography, which includes determining the electrical activity on the surface of the heart that would produce the measured torso-surface potentials. The isochrone maps illustrated in views **900**, **902**, **904**, **910**, **912** and **914** are based on images of hearts of two different patients, which are also used to determine the geometry of the heart and relationship to the corresponding torso for solving the inverse problem of electrocardiography.

The model torsos and hearts may be constructed by manual or semi-automatic image segmentation from available databases of previously acquired medical images (CT/MRI) of cardiomyopathy patients using commercially available software. Each model may be discretized using boundary element method and may be further manipulated to account for patients with different physical characteristics (e.g., large frame, medium frame and small frame) and heart sizes (e.g., x-large, large, medium, small).

A user may select the appropriate model torso and heart to suit the patient, e.g., a patient having a large torso may be simulated with a large frame model torso. In some examples, medical images of the patient, e.g., CT or MRI images, may be manually or semi-automatically segmented, registered, and compared to a variety of available models for selection from amongst the models. One or more views of 2-D

medical images (e.g., X-ray or fluoroscopy) may also be used. The user may project the measured torso-surface potentials from the torso of the patient onto the corresponding locations on the model torso. The inverse problem of propagating the electrical signals from the model torso to the model heart may then be solved, and activation times for the model heart may be estimated.

In one example in which the techniques of this disclosure were applied, human thoracic CT images for other subjects were obtained from image databases. Semi-automatic image segmentation was performed on the images to generate the three-dimensional representation of the different models of hearts and torsos. In some examples, image segmentation may be done with the AMIRA software package commercially-available from Visage Imaging, Inc., of San Diego, Calif.

For the example, the projection of electrode locations on the patient torso to the model torso was approximate. In particular, the locations electrodes on the patient torso to the model torso the locations of the electrodes on the patient torso were projected onto the surface of the model torso based on the order in which the electrodes were mounted on the patient. For the purpose of this projection, the patient and model torsos were divided into right anterior, left anterior, right posterior and left posterior regions, using the sternum (anterior) and the spine (posterior) as references. Electrodes were arranged in vertical strips and three strips were applied to each region of the torso. Electrodes in these regions were projected on to the corresponding segments of the model torso. The method described is one of many techniques that may be used to registered or map the geometrical distribution of measured electrical potentials. For example, the measured electrical potentials. For example, the measured electrical potentials may be interpolated and resampled at electrode positions given by the model. Projection of the electrode locations from segments of the patient torso onto the corresponding segments of the model torso in the correct order enabled the activation patterns and spatial dispersion of activation on the model heart to reflect the activation patterns and spatial dispersion of activation on the actual patient heart with relative accuracy. In one example, the inverse problem of electrocardiography may be solved using the Matlab regularization toolbox (Hansen PC, Regularization Tools: A Matlab package for analysis and solution of discrete ill-posed problems, Numerical Algorithms, 6(1994), pp 1-35).

Input data-sets for solving the inverse problem consistent with the example may include multi-electrode surface ECG measurements, the 3-D Cartesian coordinates of the model heart and torso surfaces, and the mesh over each model surface which specified the connectivity of the different points on each surface. An output consistent with the techniques of this disclosure may include activation times on the 3-D model heart surface which can be visualized using visualization software and computer graphics tools. In some examples, the 3-D model heart surface may be visualized using the tools in Matlab (Mathworks Inc, Natick, Mass.) or more advanced visualization software, such as Tecplot (Tecplot Inc, Bellevue, Wash.).

Comparing estimated cardiac activation times on two different, both cardiac activation times determined from the same torso-surface potential signals for one subject, show similar patterns and distribution. For example, region **906** of views **902** and **904** corresponds in size and activation time to region **916** of views **912** and **914**. Region **908** of views **902** and **904** corresponds to region **918** of views **912** and **914**. Additionally, the standard deviations of activations time for both models are both derived from the same torso-surface potentials for one subject, were similar (17.6 and 15.5 ms). The overall pattern of cardiac activation and measures of dispersion of cardiac activation times are thus not dependent on a specific heart-torso model. Using a generic heart-torso model may allow a user to create an isochrone model of the cardiac activation time suitable for diagnosis and observation while avoiding expense, inconvenience, and radiation exposure that may be caused by the CT scan or other imaging that may be used to produce a patient-specific model of the heart of the patient.

FIG. **10** is a flow diagram illustrating an example operation of a system to measure the cardiac electrical dyssynchrony of a patient via the cardiac activation times. Processing unit **500** determines the location of the electrodes **404**, e.g., based on an analysis of imaging data by an electrode location registration module **524**. Processing unit projects the locations of the electrodes onto a model torso, e.g., a selected model torso (**1002**).

A cardiac event, e.g., depolarization, occurs causing an electrical signal to propagate through the torso of the patient, and register on the electrodes distributed on the surface of the torso of the patient. The torso-surface potential signals sensed by the electrodes may be received by processing unit **500** (**1004**). The processing unit may project the signals onto the surface of the model torso based on the determined locations of the electrodes (**1006**).

The processing unit may solve the inverse problem of determining epicardial potentials based on torso-surface potentials (**1008**). The processing unit may then calculate cardiac activation times at a variety of locations of the model heart based upon the projected torso-surface potentials (**1010**). The cardiac activation times may be computed by, for example, determining the greatest negative slope of the epicardial electrogram potentials (**1016**) or by least squares minimization in the solution of the inverse problem (**1018**). The cardiac activation time may be displayed (**1012**). Examples of potential methods for displaying cardiac activation times include isochrone maps (**1014**) and a movie depicting the progression of the wavefront over the model heart (**1016**). The processing unit may be configured to allow a user select between, or display simultaneously, various display modes, including the wave front movie and isochrone maps. Additionally, one or more indices of cardiac electrical dyssynchrony may be calculated (**1018**), including the SDAT (**1020**), RAT (**1022**), and PLAT (**1024**).

For solving the inverse problem (**1008**), epicardial potentials may be computed from projected torso-surface potentials assuming a source-less volume conductor between the heart and the torso in an inverse Cauchy problem for Laplace's equation. Alternatively, an analytic relation between torso-surface potentials and the cardiac transmembrane potential may be assumed. Additionally, cardiac activation times may be estimated (**1010**) from the steepest negative slope of the epicardial electrograms determined from the inverse solution of the torso-surface potential/epicardial potential transformation. In other examples, model torso-surface potentials may be simulated based on the analytic relationship approach to determining the cardiac transmembrane potential from torso-surface potential. Cardiac activation times (parameters in the analytic relationship) may be computed based on minimizing the least square difference between the projected model torso-surface potentials and simulated torso-surface potentials.

In some examples, the construction of a torso-surface activation times isochrone map (**1014**), wavefront animation (**1016**), or other graphical representation of cardiac electrical

dyssynchrony, as well as the calculation of indices of cardiac electrical dyssynchrony (**1018**), may be performed for a particular region of the model heart based the computed cardiac activation times in such regions. Graphical representations and indices of cardiac electrical dyssynchrony may be determined for each of a plurality of regions based on the computed cardiac activation times in such regions. In some examples, the representations and indices for various regions may be presented together or compared.

FIG. **11** is a flow diagram illustrating an example technique for measuring the cardiac electrical dyssynchrony of a patient via determined cardiac activation times. The techniques may comprise determining the location of a plurality of electrodes (**1100**), projecting the location of the electrodes onto the surface of a model torso (**1102**), recording the output of the plurality of electrodes (**1104**), projecting the output of the plurality of the electrodes on the surface of the model torso (**1106**), solving the inverse problem (**1108**) and determining the cardiac activation times for a model heart from the projected torso-surface potentials (**1110**). The cardiac activation times may be displayed (**1112**). One or more indices of electrical dyssynchrony may be calculated (**1114**). The output, the indices of cardiac electrical dyssynchrony and cardiac activation time maps, may be monitored, allowing a user to diagnose the patient, adjust the position of CRT electrodes during implantation (**1118**), or adjust A-V or V-V pacing intervals of the CRT device (**1120**).

A user may monitor the output of the calculations (**1116**), e.g., the at least one indices of cardiac electrical dyssynchrony or the display of cardiac activation times. Monitoring these values may allow the user to diagnose a condition that might benefit from CRT or to evaluate the effectiveness of CRT. For example, the at least one index of cardiac electrical dyssynchrony may indicate the presence of damage to electrical conductivity of the heart of the patient, for example the presence of a left or right bundle branch block, that may not be apparent from the examination of a standard 12 lead ECG readout. A large SDAT indicates that the activation of the ventricles is occurring over a large time span, indicating that the depolarization of the ventricles is not occurring simultaneously. A large RAT also indicates a broad range of activation times and asynchronous contraction of the ventricles. A high PLAT may indicate that a specific region of the heart, e.g., the posterior regions more associated with the left ventricle, is failing to activate in concert with the measured QRS complex.

The user may adjust the positioning of CRT electrodes, e.g., electrodes **108**, **110**, and **112** of IMD **100** (FIG. **1**) according to the displayed cardiac activation times or the indices of cardiac electrical dyssynchrony. For example, the processing unit, via a display, may implement system that displays shifting colors based on the percentage change of the indices of cardiac electrical dyssynchrony. As the position of the CRT electrodes are adjusted (**1118**), the displayed colors may shift from red to yellow to green based on the percentage improvement of the indices of cardiac electrical dyssynchrony. This may allow a user to rapidly determine if the adjustments of the CRT electrodes are having a positive effect on the symptoms of the patient. In another example, the user may adjust the A-V or V-V pacing intervals of an implanted CRT device (**118**). The minimum value of the indices of cardiac electrical dyssynchrony may indicate adequate pacing intervals. Isochrone maps or wave front propagation movies may also be used to aid in CRT adjustments or to diagnose conditions that may be responsive to CRT treatment.

As indicated above, to facilitate evaluating the whether a patient is a candidate for CRT based on the monitored output (**1116**), the one or more indications of cardiac electrical dyssynchrony, e.g., indices or graphical indications, may be determined based on torso-surface activation times during both intrinsic conduction of the heart, and during CRT. Differences between the indications during intrinsic conduction and CRT may indicate that CRT would provide benefit for the patient, e.g., that the patient is a candidate for CRT. Furthermore, during implantation or a follow-up visit, the one or more indications of cardiac electrical dyssynchrony may be determined for each of a plurality of lead positions, electrode configurations, or other parameter values based on torso-surface activation times resulting from delivery of CRT at the positions, or with the electrode configurations or parameter values. In this manner, differences between cardiac electrical dyssynchrony indications associated with various locations, electrode configurations, or parameter values may be compared to determine preferred locations, configurations, or values.

Various examples of this disclosure have been described. However, one of ordinary skill in the art will appreciate that various modifications may be made to the described embodiments without departing from the scope of the claims. For example, although SDAT, RAT and PLAT have been discussed as example statistical indices of the dispersion of activation times, other indices or metrics of the dispersion of the timing of depolarization may be determined according the techniques of this disclosure. As one example, a range of activation times between two specific regions, e.g., anterior and posterior, may be determined. As another example, a range or variability of activation times after excluding certain locations or regions may be determined according to the techniques of this disclosure. The excluded locations or regions may be those that are believed to be scar tissue, e.g., identified by low amplitude electrical signals, or locations or regions that are beyond the extent of the far-field QRS complex. In general, calculation of an index may include determining any statistical or other value based on the torso-surface or cardiac activation times, or some subset thereof. These and other examples are within the scope of the following claims.

The invention claimed is:

1. A method comprising:

receiving, with a processing unit, a torso-surface potential signal from each electrode of a plurality of electrodes distributed on a torso of a patient, wherein receiving the torso-surface potential signal from each electrode comprises:

receiving first torso-surface potential signals sensed during intrinsic conduction of the heart of the patient; and

receiving second torso-surface potential signals sensed during cardiac resynchronization therapy (CRT) pacing of the heart of the patient;

for each electrode of at least a subset of electrodes of the plurality of electrodes, calculating, with the processing unit, a torso-surface activation time based on the torso-surface potential signal sensed from the electrode, wherein calculating the torso-surface activation times comprises:

calculating first torso-surface activation times based on the first torso-surface potential signals; and

calculating second torso-surface activation times based on the second torso-surface potential signals, and

determining, with the processing unit, an indication of a degree of electrical dyssynchrony of a heart of the

patient based on the calculated torso-surface activation times, wherein the indication comprises a value that quantifies the degree of electrical dyssynchrony of the heart, and wherein determining the indication of the degree of electrical dyssynchrony of the heart of the patient based on the calculated torso-surface activation times comprises determining a change in electrical dyssynchrony between first torso-surface activation times and the second torso-surface activation times; and

presenting, by the processing unit, to a user, the indication of the degree of electrical dyssynchrony via a display, wherein presenting the indication of the degree of electrical dyssynchrony comprises presenting an indication of the change in electrical dyssynchrony.

2. The method of claim **1**, wherein determining the indication of the degree of electrical dyssynchrony of the heart of the patient based on the calculated torso-surface activation times further comprises calculating at least one index of electrical dyssynchrony of the heart based on the torso-surface activation times, the indication comprising the index of electrical dyssynchrony, and wherein presenting the indication of the degree of electrical dyssynchrony comprises presenting the calculated index to the user.

3. The method of claim **2**, further comprising:

comparing, with the processing unit, the first torso-surface activation times during intrinsic conduction of the heart to the second torso-surface activation times during CRT pacing of the heart,

wherein calculating the at least one index of electrical dyssynchrony comprises calculating the at least one index of electrical dyssynchrony based at least on comparing the first torso-surface activation times during intrinsic conduction of the heart to the second torso-surface activation times during CRT pacing of the heart.

4. The method of claim **2**, wherein calculating the at least one index of electrical dyssynchrony comprises calculating a standard deviation index (SDAT) computed as a standard deviation of the torso-surface activation times.

5. The method of claim **2**, wherein calculating the at least one index of electrical dyssynchrony comprises calculating a range of activation times (RAT), wherein calculating the RAT comprises:

determining a maximum of the torso-surface activation times;

determining a minimum of the torso-surface activation times; and

determining a difference between the maximum of the torso-surface activation times and the minimum of the torso-surface activation times.

6. The method of claim **2**, wherein calculating the at least one index of electrical dyssynchrony comprises calculating a percentage of late activation times (PLAT), wherein calculating the PLAT comprises:

determining a QRS complex duration; and

determining a percentage of the torso-surface activation times within a region of the torso that are later than a percentage of the QRS complex duration.

7. The method of claim **2**, wherein calculating the at least one index of electrical dyssynchrony comprises:

calculating a first index of electrical dyssynchrony for a first region of the torso based on torso-surface activation times from the first region of the torso; and

calculating a second index of electrical dyssynchrony for a second region of the torso based on torso-surface activation times from the second region of the torso.

8. The method of claim **2**, wherein calculating the at least one index of electrical dyssynchrony comprises:

calculating a first set of two or more indices of electrical dyssynchrony for a first region of the torso based on torso-surface activation times from the first region of the torso; and

calculating a second set of two or more indices of electrical dyssynchrony for a second region of the torso based on torso-surface activation times from the second region of the torso.

9. The method of claim **2**, wherein calculating the at least one index of electrical dyssynchrony comprises, for each of several regions of the torso, calculating a set of two or more indices of electrical dyssynchrony for the region of the torso based on torso-surface activation times from region of the torso.

10. The method of claim **1**, wherein presenting the indication of the degree of electrical dyssynchrony of the heart of the patient further comprises:

calculating a torso-surface activation time isochrone map based on the calculated torso-surface activation times, wherein the isochrones map depicts a spatial distribution of torso-surface activation times; and

presenting the torso-surface activation time isochrone map via the display.

11. The method of claim **1**, wherein presenting the indication of the degree of electrical dyssynchrony of the heart of the patient further comprises:

calculating a wave front animation based on the calculated torso-surface activation times, wherein the wave front animation depicts a spatial progression of the activation of the heart; and

presenting the wave front animation via the display.

12. The method of claim **1**, wherein presenting the indication of the degree of electrical dyssynchrony of the heart of the patient comprises displaying one of a plurality of predefined colors, each of the colors indicating a respective degree of the change of electrical dyssynchrony.

13. The method of claim **1**, wherein presenting the indication of the degree of electrical dyssynchrony of the heart of the patient comprises presenting the indication during an implantation procedure for a cardiac resynchronization therapy (CRT) device.

14. The method of claim **1**, wherein presenting the indication of the degree of electrical dyssynchrony of the heart of the patient comprises presenting the indication during an adjustment procedure for a cardiac resynchronization therapy (CRT) device.

15. The method of claim **1**, wherein presenting the indication of the degree of electrical dyssynchrony of the heart of the patient comprises presenting the indication during a screening procedure to determine if a given patient might benefit from implantation of a cardiac resynchronization therapy (CRT) device.

16. The method of claim **1**, wherein calculating, for each electrode of the at least the subset of electrodes, the torso-surface activation time comprises determining an electrical activation time of a region of the heart of the patient associated with the electrode based on the torso-surface potential signal received from the electrode.

17. The method of claim **16**, wherein determining the electrical activation time of the region of the heart of the patient associated with the electrode based on the torso-surface potential signal comprises solving an inverse problem of electrocardiography.

18. A system comprising:

a plurality of electrodes distributed on a torso of a patient; and

a processing unit configured to receive a torso-surface potential signal from each electrode of the plurality of electrodes, calculate, for each electrode of at least a subset of electrodes of the plurality of electrodes, a torso-surface activation time based on the torso-surface potential signal sensed from the electrode, and determine an indication of a degree of electrical dyssynchrony of a heart of the patient based on the calculated torso-surface activation times, wherein the indication comprises a value that quantifies the degree of electrical dyssynchrony of the heart,

wherein the torso-surface potential signal comprises first torso-surface potential signals sensed during intrinsic conduction of the heart of the patient and second torso-surface potential signals sensed during cardiac resynchronization therapy (CRT) pacing of the heart of the patient, wherein the processing unit is configured to calculate the torso-surface activation times by at least calculating first torso-surface activation times based on the first torso-surface potential signals and calculating second torso-surface activation times based on the second torso-surface potential signals, and wherein the indication of the degree of dyssynchrony comprises an indication of a change in electrical dyssynchrony between first torso-surface activation times and the second torso-surface activation times.

19. The system of claim 18, further comprising a display, wherein the processing unit is further configured to:

calculate at least one index of electrical dyssynchrony of the heart based on the torso-surface activation times, the indication comprising the index of electrical dyssynchrony; and

present the calculated index to a user via the display.

20. The system of claim 19, wherein the processing unit is further configured to:

compare the first torso surface activation times during intrinsic conduction of the heart to the second torso-surface activation times during CRT pacing of the heart; and

calculate the at least one index of electrical dyssynchrony based at least on comparing the first torso surface activation times during intrinsic conduction of the heart to the second torso-surface activation times during CRT pacing of the heart.

21. The system of claim 19, wherein the at least one index of electrical dyssynchrony comprises a standard deviation index (SDAT), and wherein the processing unit is configured to calculate the standard deviation index (SDAT) by at least determining a standard deviation of the torso-surface activation times.

22. The system of claim 19, wherein the at least one index of electrical dyssynchrony comprises a range of activation times (RAT), and wherein the processing unit is configured to calculate the range of activation times (RAT) by at least determining a maximum of the torso-surface activation times, determining a minimum of the torso-surface activation times, and determining a difference between the maximum of the torso-surface activation times and the minimum of the torso-surface activation times.

23. The system of claim 19, wherein the at least one index of electrical dyssynchrony comprises a percentage of late activation times (PLAT), and wherein the processing unit is configured to calculate the percentage of late activation times (PLAT) by at least determining a QRS complex duration and determining a percentage of subset of the torso-surface activation times within a region of the torso that are later than a percentage of the QRS complex duration.

24. The system of claim 19, wherein the processing unit is configured to:

calculate a first index of electrical dyssynchrony for a first region of the torso based on torso-surface activation times from the first region of the torso; and

calculate a second index of electrical dyssynchrony for a second region of the torso based on torso-surface activation times from the second region of the torso.

25. The system of claim 19, wherein the processing unit is configured to:

calculate a first set of two or more indices of electrical dyssynchrony for a first region of the torso based on torso-surface activation times from the first region of the torso; and

calculate a second set of two or more indices of electrical dyssynchrony for a second region of the torso based on torso-surface activation times from the second region of the torso.

26. The system of claim 18, further comprising a display, wherein the processing unit is configured to:

calculate a torso-surface activation time isochrone map based on the calculated torso-surface activation times, wherein the isochrones map depicts a spatial distribution of torso-surface activation times; and

present the torso-surface activation time isochrone map via the display.

27. The system of claim 18, further comprising a display, wherein the processing unit is configured to:

calculate a wave front animation based on the calculated torso-surface activation times, wherein the wave front animation depicts a spatial progression of the activation of the heart; and

present the wave front animation via the display.

28. The system of claim 18, wherein the processing unit is configured to present the indication of the degree of electrical dyssynchrony by at least displaying, via the display, one of a plurality of predefined colors, each of the colors indicating a respective degree of the change of electrical dyssynchrony of the heart of the patient.

29. The system of claim 18, wherein the processing unit is configured to calculate, for each electrode of the at least the subset of electrodes, the torso-surface activation time by at least determining an electrical activation time of a region of the heart of the patient associated with the electrode based on the torso-surface potential signal received from the electrode.

30. The system of claim 18, further comprising a display, wherein the processing unit is configured to present to a user, via the display, the indication of the degree of dyssynchrony of the torso-surface activation times.

31. A non-transitory computer-readable storage medium comprising instructions that, when executed, cause a processor to:

receive a torso-surface potential signal from each electrode of a plurality of electrodes distributed on a torso of a patient by at least:

receiving first torso-surface potential signals sensed during intrinsic conduction of the heart of the patient; and

receiving second torso-surface potential signals sensed during cardiac resynchronization therapy (CRT) pacing of the heart of the patient;

calculate, for each electrode of at least a subset of electrodes of the plurality of electrodes, a torso-surface activation time based on the torso-surface potential signal sensed from the electrodes, wherein the instruc-

tions, when executed, cause the processor to calculate the torso-surface activation time by at least:

calculating first torso-surface activation times based on the first torso-surface potential signals; and

calculating second torso-surface activation times based on the second torso-surface potential signals;

determine an indication of a degree of electrical dyssynchrony of a heart of the patient based on the calculated torso-surface activation times, wherein the indication comprises a value that quantifies the degree of electrical dyssynchrony of the heart wherein the instructions, when executed, cause the processor to determine the indication of the degree of electrical dyssynchrony by at least determining a change in in electrical dyssynchrony between first torso-surface activation times and the second torso-surface activation times; and

present to a user, the indication of the degree of electrical dyssynchrony via a display by at least presenting an indication of the change in electrical dyssynchrony.

32. The non-transitory computer-readable medium of claim **31**, wherein the instructions, when executed, cause the processor to calculate, for each electrode of the at least the subset of electrodes, the torso-surface activation time by at least determining an electrical activation time of a region of the heart of the patient associated with the electrode based on the torso-surface potential signal received from the electrode.

* * * * *

专利名称(译)	评估心脏内激活模式和电不同步		
公开(公告)号	US9510763	公开(公告)日	2016-12-06
申请号	US13/462404	申请日	2012-05-02
[标]申请(专利权)人(译)	美敦力公司		
申请(专利权)人(译)	美敦力公司，INC.		
当前申请(专利权)人(译)	美敦力公司，INC.		
[标]发明人	GHOSH SUBHAM GILLBERG JEFFREY M STADLER ROBERT W		
发明人	GHOSH, SUBHAM GILLBERG, JEFFREY M. STADLER, ROBERT W.		
IPC分类号	A61B5/04 A61N1/362 A61B5/0452 A61B5/05 A61B5/02 A61B5/0402 A61B5/0408 A61B5/00 A61N1/368 A61N1/04		
CPC分类号	A61B5/04012 A61B5/02 A61B5/0402 A61B5/0452 A61B5/04085 A61B5/05 A61B5/742 A61N1/0476 A61N1/0484 A61N1/3627 A61N1/3682 A61N1/3684 A61N1/36842 A61N1/36843 A61B5/044		
优先权	61/482053 2011-05-03 US		
其他公开文献	US20120283587A1		
外部链接	Espacenet USPTO		

摘要(译)

描述了用于评估心脏电动不同步的技术。在一些示例中，为多个躯干表面电位信号中的每一个确定激活时间。可以分析或呈现这些激活时间的分散或序列，以提供患者心脏的电不同步的多种指示。在一些示例中，该组电极的电极的位置以及因此感测到躯干表面电位信号的位置可以被投影在包括模型心脏的模型躯干的表面上。可以解决心电图的逆问题，以基于从患者感测的躯干表面电位信号来确定模型心脏的区域的电激活时间。